In: Problems of Biosphere Origin and Evolution. Volume 2 ISBN: 978-1-62808-346-0
Editor: E. M. Galimov

Chapter 3

IMPULSIVE HEATING OF GAS-DUST NEBULAR CONDENSATES AS A MECHANISM FOR THE CONJUGATE FORMATION OF SILICATE CHONDRULES AND METAL

A. A. Ariskin**, O. I. Yakovlev, K. A. Bychkov, G. S. Barmina and G. S. Nikolaev
Vernadsky Institute of Geochemistry and Analytical Chemistry,
Russian Academy of Sciences, Russia

ABSTRACT

We present an updated version of the METEOMOD model (2008) that allows the compositional evolution of chondritic systems during Fe-Ni metal reduction when heating the starting material above the silicate liquidus to be calculated (*Ariskin et al*., 2007; *Bychkov et al*., 2006). Calculations using this model showed a similarity of the calculated metal proportions and composition of the complementary silicate melt to those of ordinary chondrites. This was an argument for the hypothesis that the variations in maximum temperatures during heating the protochondritic systems above the olivine liquidus were responsible for the different degrees of metal and silicate chondrule reduction (*Ariskin et al.*, 1997). The formation of metal and proto-chondrule melts by thermal reduction does not depend on the redox conditions in the gas-dust nebula. The reduction factor is the temperature increase, which causes the metal solubility in the melt to decrease. To support this hypothesis, we performed a series of low-pressure calculations simulating the thermal reduction of solar-composition gas condensates in the presence of primordial dust. The calculations were carried out on mineral compositions representing the condensation products of the solar nebula at 800–1200 K (based on the Petaev-Wood condensation model, the CWPI code). These compositions were subjected to "numerical heating" above the olivine liquidus at ~1550–2100° C and constant oxygen fugacity (log f_{O2} = –6.5). As a result, a progressive metal release was observed coupled with the formation of a sequence of FeO-depleted and SiO_2-enriched residual melts

* email: ariskin@geokhi.ru.

demonstrating a monotonous increase in mg#. A nontrivial result of these calculations is that the model relations between the amount and composition of the Fe-Ni metal turned out to be identical to the observed metal characteristics in ordinary LL, L, and H chondrites. Thus, impulsive heating of a protochondritic material could be an important factor of the early high-temperature differentiation and formation of primary metallic phases and complementary silicate spherules.

FORMULATION OF THE PROBLEM[1]

In the early 1980s, King (1982, 1983) experimentally studied the thermal action of a concentrated solar beam on samples of meteorites and terrestrial basalts. Rapid heating of these materials in a low vacuum to temperatures above 2000° C gave rise to large drops of an immiscible metallic phase as a result of local iron reduction from a silicate liquid. Such phenomena found analogies with the results of previous peridotite melting experiments in a high-frequency setup at 1700° C in an argon atmosphere (*Barmina et al.*, 1974). Efficient metal reduction was also observed in melting and evaporation experiments on the Krymka, Saratov, and Murchison meteorites (*Yakovlev et al*., 1985, 1987, 2003). This process was called *thermal reduction* (*Yakovlev et al*., 1987). The presented experimental data found further confirmation in the results of thermodynamic calculations based on the METEOMOD model (*Ariskin et al*., 1997), which was applied to the compositional evolution of chondritic systems when the starting material was successively heated and reduced at temperatures 1570–2100° C (*Ariskin et al.*, 1997). Calculations using an updated version of this model (*Bychkov et al*., 2006) showed a similarity of the calculated proportions and composition of the thermal reduction products (both the metal and silicate melt) to those of the mineral phases in some types of ordinary chondrites (*Ariskin et al*., 2006). This suggested that the heating of the protochondritic source at temperatures above the silicate liquidus could be considered as an important factor that gives rise to a mineral-chemical peculiarity of silicate chondrules and regular variations in metal composition (*Yakovlev et al*., 2008). Accepting the reality and analyzing the geochemical peculiarities of this mechanism lead us to the paradoxical conclusion that the differences in redox conditions in the solar nebula might not play a crucial role in the metal reduction processes. The degree of reduction of the metallic phase from the primitive "solar" source was determined not by the scales of deviations of the redox conditions from the iron-wüstite (IW) buffer but mainly by the heating rate and the amplitude of the corresponding temperature jump. During rapid heating to temperatures 1600–2000° C, the presence of a reducing agent (carbon, hydrogen) is not a necessary condition for the formation and separation of the metallic phase from a molten protochondritic material.

[1] We are grateful to A.A. Borisov who developed the silicate-metal equilibrium equations in the early 1990s based on which it has become possible to construct the first mafic to ultramafic magma crystallization models by taking into account the metallic phase separation. We are also thankful to M.I. Petaev who kindly provided a Fortran code of the CWPI program for GDN condensation calculations and gave a number of valuable remarks on the content of the paper. This work was supported by the Basic Research Program no. 18 of the Presidium of the Russian Academy of Sciences ("Problems of the Formation of the Earth's Biosphere and Its Evolution").

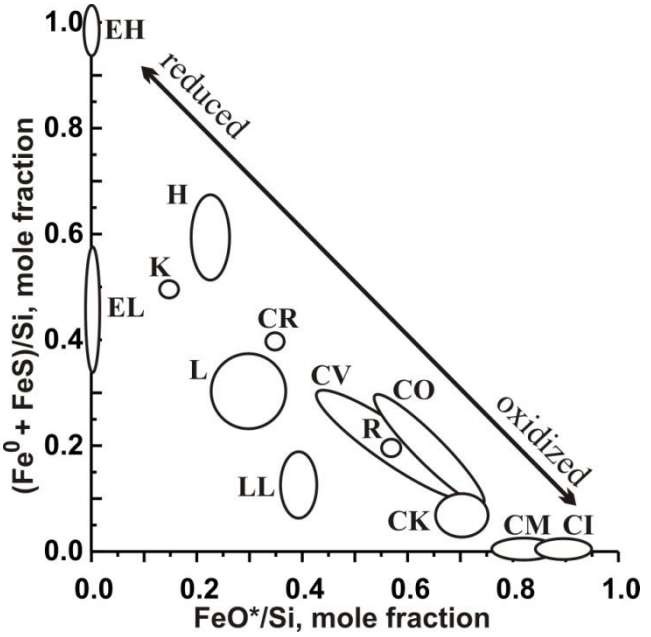

Figure 1. Oxidation state diagram for various groups of chondrites from Krot et al. (2003). The relative content of reduced iron in the form of metal and sulfide is plotted versus the iron content in silicates and oxides.

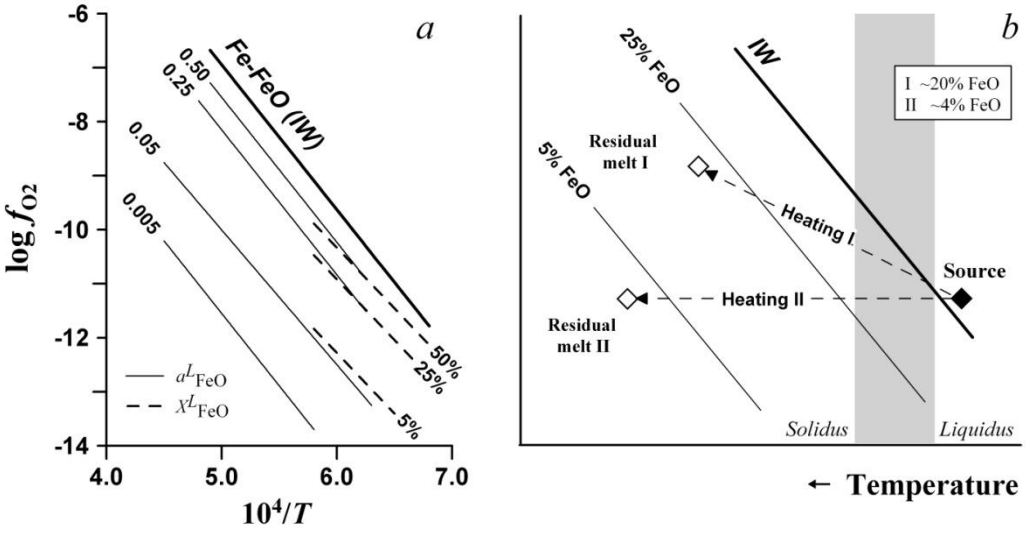

Figure 2. (a) Graphs of the isopleths of FeO activity and solubility in silicate melts and (b) schematic diagram of metallic iron reduction from a protochondritic source. The line of IW buffer equilibrium and the isopleths of FeO activity were estimated from (7) based on thermochemical data for the iron oxide decomposition reaction (*Myers and Eugster*, 1983); the lines of equal FeO solubility were calculated using an empirical equation (*Ariskin et al.*, 1992). The arrows in Fig. 2b represent the possible heating trajectories that bring the figurative point of the initial composition to the corresponding isopleth of solubility in the super-liquidus region (25 % FeO). Further heating suggests successive metal reduction with the formation of residual melts (as the source of silicate chondrules?) variously depleted in FeO and enriched in SiO_2 (normative enstatite).

Such a formulation of the problem allows us to take a fresh look at one of the paradigms of meteoritics stating that the formation of ordinary chondrites in the sequence $LL \rightarrow EH$ was controlled by the transition to more reducing conditions (see, e.g., *Rubin et al.*, 1988). Here, it is pertinent to recall that since the paper by Prior (1916), the ratio of the metallic and oxide forms of iron is a universally accepted criterion for the separation of chondrites by the redox state. The higher the metal content and the less ferrous the coexisting olivine and pyroxene in a chondrite, the more reduced it is (Prior's first rule). Enstatite and carbonaceous chondrites have been considered, respectively, as the most reduced and most oxidized groups of chondrites (Fig. 1). This understanding of the chondrite compositions gave rise to the genetic concept of the existence of zones with various redox conditions in the protosolar nebula, where the various types of chondrites were formed. According to Nagahara (1986), the differences in redox conditions for the formation of E-chondrites and C-chondrites are ~10 orders of magnitude of f_{O2}. It should also be noted that there was probably no metallic iron in the primordial material of the protosolar nebula itself. The composition of the most primitive objects in the solar system, carbonaceous CI chondrites containing no metallic iron, serves as a basis for this conclusion. These chondrites apparently represent compacted interstellar dust that has not undergone even weak heating (> 100° C) over the entire history of its existence (*Simonenko*, 1985). The absence of chondrules in carbonaceous CI chondrites also suggests that there is no evidence of heating and melting. It can be hypothesized that the metal, along with the chondrules, could be formed in a unified process of heating of this primordial dust above the melting temperature.

The proposed concept of thermal reduction of protochondritic materials allows the amount of metal, the variations of its composition, and the degree of reduction of the silicates to be related to the various degrees of heating of the starting material under an impulsive thermal action. Thus, the conjugacy and complementarity of the formation of the silicate and metallic components of ordinary chondrites can be naturally explained (see, e.g., *Kong and Ebihara*, 1997; *Connoly et al*., 2001; *Campbell et al*., 2005). As will be shown below, the amount and composition of the metal produced in such processes are controlled by a heating amplitude of ~ 400–500° C.

THEORETICAL BACKGROUND AND DEVELOPMENT OF THE METEOMOD MODEL

A thermodynamic analysis shows that the process of successive phase separation (mineral crystallization or immiscible liquid segregation) in isobaric-isothermal systems as the temperature drops is controlled by a partial change in the Gibbs free energy relative to the amount of a specified phase precipitating from the melt (see, e.g., *Frenkel et al.*, 1988; *Ariskin and Barmina*, 2000):

$$\partial G/\partial n = -\Delta H\,(T_2/T_1 - 1), \qquad (1)$$

where $n > 0$ is the amount of mineral or liquant, ΔH is the enthalpy of the corresponding phase transition, and the equilibrium temperatures T_1 and T_2 represent the initial and current states of the heterogeneous system. Since the silicate crystallization reactions are exothermic,

where $\Delta H_{cr} < 0$ is usually varies between –60 and –140 kJ/mole (*Bouhifd et al.*, 2007), the increase in the degree of crystallization of the system ($\partial n > 0$) during temperature decrease ($T_2 < T_1$) is a spontaneous process characterized by a decrease in the system's free energy ($\partial G < 0$).

The situation with the thermochemical description of iron crystallization or liquation is different:

$$FeO(L) = Fe^0 + 0.5O_2. \quad (2)$$

The solid/liquid oxide decomposition reactions are known to require expending a large amount of heat. In particular, for the temperature range 1600–2100 K, the enthalpy of the reaction $FeO_{solid} = Fe^0 + 0.5O_2$ based on the DIANIK database (*Shapkin and Sidorov*, 2004) varies between 267 and 255 kJ/mole. Obviously, the precipitation of zero-valent iron from a silicate melt is also a highly endothermic process. In this case, reaction (2), which suggests a decrease in the system's free energy as the amount of reduced metal increases ($\partial n > 0$),

$$\partial G/\partial n = -\Delta H_{FeO} (T_2/T_1 - 1) < 0, \quad (3)$$

is possible in principle under the condition $T_2/T_1 - 1 > 0$, which is equivalent to a rise in the temperature ($T_2 > T_1$). Thus, the experimentally established effects of thermal reduction of iron from basalts and ultrabasic materials (*Barmina et al.*, 1974; *King*, 1982, 1983; *Yakovlev et al.*, 1987, 2003) are thermodynamically substantiated as resulting from the absorption of heat (energy) by the system accompanied by the increase in the temperature. Basically, this conclusion confirms the well-known empirical observation that the solubility of transitional metals in silicate melts at constant oxygen fugacity decreases with increasing temperature (see, e.g., *Holzheid et al.*, 1994).

The isopleths of FeO solubility (activity) in a melt presented in Fig. 2a in oxygen fugacity-temperature coordinates can serve as a graphical expression of these relationships and an illustration of the expected thermal reduction effects. We plotted these graphs based on two sources of information. The line of iron-wüstite (IW) buffer equilibrium is given on the basis of thermochemical calculations (*Myers and Eugster*, 1983)

$$\log f_{O2} = -26834.7/T + 6.471. \quad (4)$$

These were also used to plot the isopleths of FeO activity (thin lines) based on the expressions for the equilibrium constant of reaction (2):

$$\log K_{(2)} = \log(a_{Fe0}) + 0.5\log f_{O2} - \log(a^L_{FeO}) == -\Delta G_{FeO}/2.303RT, \quad (5)$$

$$2\log K_{(2)} = -2\Delta G_{FeO}/2.303RT = -2\Delta H_{FeO}/2.303RT ++ 2\Delta S_{FeO}/2.303R, \quad (6)$$

in the approximation of $a_{Fe}0 = 1$:

$$\log f_{O2} = 2[\log K_{(2)} + \log (a^L_{FeO})] = -26834.7/T ++ 6.471 + 2\log (a^L_{FeO}). \quad (7)$$

The dashed lines in Fig. 2a characterize the FeO solubility in silicate melts (X^L_{FeO}) estimated using an empirical equation constructed from the results of 396 experiments at temperatures 1150–1327° C (*Roeder*, 1974; *Doyle and Naldrett*, 1986; *Doyle*, 1988) and proposed by Ariskin et al. (1992). Comparison of these data points to a consistency of the thermochemical and experimental information. This manifests itself in the presence of subparallel trends of variation in X^L_{FeO} and a^L_{FeO} and their coincidence or closeness for the temperature range in which this empirical dependence was calibrated.

The thermodynamic relations shown schematically in Fig. 2b reproduce the fundamental character of this relationship between log f_{O2}, the reciprocal temperature, and the FeO content in a silicate liquid, see Eqs. (2)–(7). In this case, the chemical consequences of the possible thermal iron reduction from an ultrabasic source during its impulsive heating manifest themselves. The two dashed arrows on this graph indicate the directions of the change in intensive parameters if the conditions of constant or variable oxygen fugacity are assumed. In both cases, it is implied that the temperature begins to rise from the solid state of the initial system and that the heating line crosses the heterogeneous region and extends into the field of the silicate melt (Fig. 2b). Suppose that the source contained 25 wt.% FeO. Depending on the amplitude of the temperature jump, the heating line can fall on the isopleth of solubility corresponding to 25 wt.% FeO in a silicate liquid at certain T-f_{O2} parameters. The point of intersection with this isopleth for each trajectory corresponds to thermodynamic equilibrium of the incipient metallic phase and the initial-composition melt. Further heating along the specified trajectory means that the figurative point falls into the metastable region of the isopleths of lower FeO solubility. Thus, the heating of the initial system can continue only in the regime of reduction of some amount of iron from the melt, in accordance with the thermochemical constraints (2)–(7).

These illustrations clearly show metal reduction complementarity and residual melt evolution under conditions when the lines of temperature rise intersect the isopleths of FeO solubility in the direction of $X^L_{FeO} = 0$. The graphs in Fig. 2b also allow us to formulate preliminary conclusions about the possible metal reduction scales. Obviously, the heating trajectory II (log f_{O2} = const) shown here gives an example of more efficient metallic phase separation, because the corresponding isopleth of solubility is reached at a lower temperature than that for trajectory I. Developing this logic, we conclude that the heating along the T-f_{O2} trajectories parallel to the IW buffer should not lead to metal reduction at all. The regime of heating (not shown here) in which the oxygen fugacity decreases with increasing temperature should have been recognized as the most efficient way of metallic phase separation. Thus, the amount of reduced metal is determined by the T-f_{O2} trajectory and the degree of superheating of the initial melt relative to the maximum permissible iron solubility for each specific composition. The presence of a reducing agent in this scheme plays no crucial role. At known contents of carbon in the dust and hydrogen in the surrounding gas, the role of these components can be reduced to the binding of oxygen produced by the thermal reduction of iron (2). It can also be assumed that the oxygen being released during heating under conditions of an open condensed system (by the system we will mean the primordial dust of the nebula) disperses in a tenuous gas medium. Thus, we proceed from the assumption that rapid (impulsive) heating of the dust component of the initial gas-dust nebula (GDN) did not lead to significant changes in the proportions of gas components and the conditions $f_{O2} \approx$ const were the most realistic regime of thermal reduction. These principles were realized in the first version of the METEOMOD computer program designed to simulate the

precipitation of metallic iron from (proto)chondritic sources at temperatures above the silicate liquidus (*Ariskin et al.*, 1997).

PRELIMINARY CALCULATIONS

The technique for simulating the effects of thermal reduction according to reaction (2) can consist in calculating the amount of iron at a given (increasing) melt temperature or predicting a temperature rise as the metallic phase is successively reduced. The second method turns out to be more convenient, because the METEOMOD program we developed (*Ariskin et al.*, 1997) solves the equilibrium problem not at a given temperature but at a fixed ratio of the residual melt and the mineral phases precipitated from it according to the algorithm presented in Frenkel et al. (1988). Adding the empirical equation for the FeO solubility (*Ariskin et al.*, 1992) to this model allowed us to perform a series of test calculations simulating the thermal reduction of iron from a melt whose composition corresponded to the annealed sample of the Saint Severin LL chondrite (*Jurewicz et*., 1995). These calculations were performed under constant oxygen pressure log $f_{O2} = -10$, which was chosen in such a way that the first portions of the metallic phase turned out to be in equilibrium with the initial liquid at a temperature slightly above than the silicate liquidus – about 1570° C (Fig. 3). The simulation results showed that more than 90 % of the metal is precipitated at temperatures exceeding the olivine liquidus by 400–500° C at constant f_{O2}. Complementary SiO_2 enrichment in the melt was also observed, causing the content of normative *Opx* to increase and the residual melt to evolve towards iron-free ("enstatite-like") compositions (*Ariskin et al.*, 1997). These results demonstrated a certain analogy in the compositional evolution of the modeled melts and the bulk compositions of the silicate component of ordinary chondrites (FeO depletion, normative *Opx* enrichment, general trend to more reduced chondrites, etc.). However, further development of the model requires an additional argumentation based on available geochemical data. Given the link of this chemical evolution with the metal precipitation process, we focus attention on the behavior of siderophile elements. Below, we will present results based on our ability to simulate the compositional evolution during the precipitation of Fe-Ni alloys.

Allowance for the Metal Composition Variability

To resolve this problem, results of an additional calibration of the METEOMOD model were used. These allow the empirical dependences for the FeO and NiO solubility in silicate melts (*Ariskin et al.*, 1996; *Borisov and Ariskin*, 1996) and the thermodynamic model of the Fe and Ni activity in Fe-Ni alloys in a wide range of compositions (*Tomiska and Neckel*, 1985) to be combined in a special “metal-melt” subroutine. We recalibrated the equation for the FeO solubility based on the same set of 396 experiments carried out at atmospheric pressure in the range $-14.5 < \log f_{O2} < -11.0$ (*Roeder*, 1974; *Doyle and Naldrett*, 1986; *Doyle*, 1988), see above. The experimental data on the NiO solubility included the results of 33 experiments on the natural compositions in nickel-enriched Fe-Ni capsules (*Campbell et al*., 1979; *Snyder and Carmichael*, 1992) and 22 experiments on the compositions of Di-An

eutectics in equilibrium with metallic Ni (*Holzheid et al.*, 1994). These experiments were conducted at P = 1 atm, temperatures 1122–1437° C, and relatively oxidizing conditions –12.6 < log f_{O2} < –8.2. The Ni content in the experimental melts was varied by three orders of magnitude. These calibrations are different from the approach in Ariskin et al. (1992) by the data parameterization technique. The latter was based on the equation

$$\log (X^{L}_{MeO} / a^{M}_{Me}) - 0.5 \log f_{O2} = h/T(\mathrm{K}) + d_i X_i, \quad (8)$$

where X^{L}_{MeO} is the FeO or NiO content in the melt (mol.%), a^{M}_{Me} is the Fe or Ni activity in the metal from the model by Tomiska and Neckel (1985), and the regression parameters h and d_i allowed for the liquid temperature and composition effects (when recalculated to iron-free and nickel-free matrix, mol.%). When separating the total iron into the proportions of Fe^{3+} and Fe^{2+} cations in the melt, we used an empirical equation from Borisov and Shapkin (1989). The corresponding regression parameters are given in Table 1.

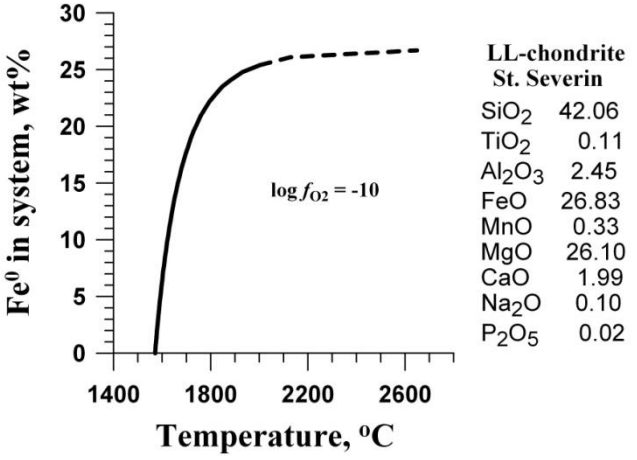

Figure 3. Amount of metal produced by the thermal reduction of a chondritic melt versus temperature of the complementary residual liquid. The initial composition corresponds to the annealed (with a lower content of volatiles) Saint Severin LL chondrite. The calculations were performed using the METEOMOD program (*Ariskin et al.*, 1997) for constant oxygen fugacity (log f_{O2} = –10). The initial composition of this chondrite is given in Table 6.

Table 1. Regression constants h and d_i in Eq. (8) to describe the FeO and NiO solubility in silicate melts (*Borisov and Ariskin*, 1996)

Parameters	**FeO equation (n = 396)**	**NiO equation (n = 55)**
1/T, K	11185.7 (158.7)	7771.7 (9095)
log f_{O2}	0.5	0.5
SiO_2	0.00357 (0.00100)	–0.01223 (0.00452)
TiO_2	0.01045 (0.00149)	0.02683 (0.01505)
Al_2O_3	0.00301 (0.00176)	0.02419 (0.01146)
MgO	0.00172 (0.00107)	0.00275 (0.00934)
CaO	–0.00411 (0.00147)	–0.00950 (0.00586)
Na_20	–0.02027 (0.00374)	–0.04076 (0.04048)
K_2O	–0.03894 (0.00247)	–0.05223 (0.02598)

The standard deviations (1σ) are given in parentheses.

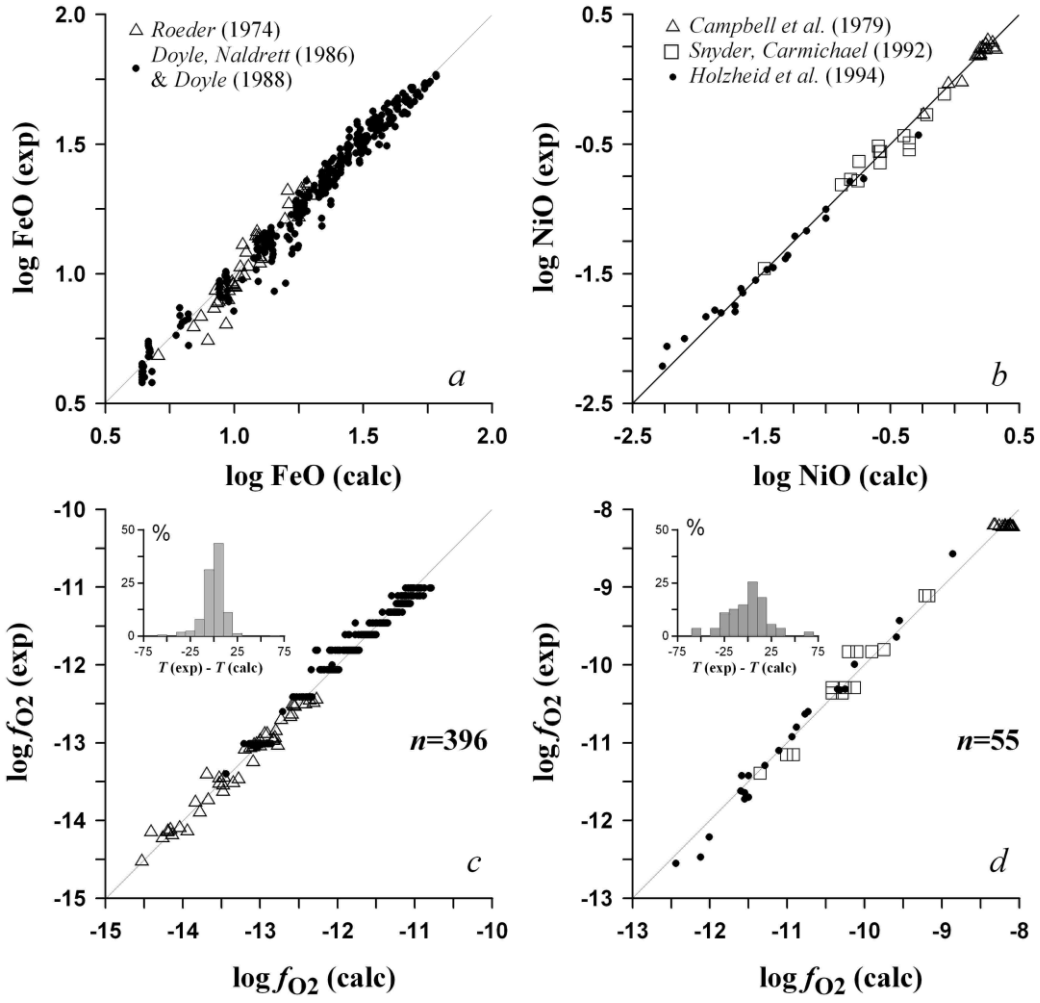

Figure 4. The results of testing the accuracy of the equations for the FeO and NiO solubility in silicate melts (8) for the contents of these oxides, log f_{O2}, and the temperature (*Borisov and Ariskin*, 1996). The calculations using the parameters from Table 1: the calculations for FeO and NiO are on the left and the right, respectively. The standard deviations when solving the inverse problem (1σ): (a) 0.035, (b) 0.049, (c) 0.070, (d) 0.097.

Figure 4 displays the results of testing the accuracy of these equations by solving the inverse problem for the selected experimental dataset. Figures 4a and 4b compare the observed and modeled NiO and FeO contents in the melts at fixed temperature, log f_{O2}, and metal and silicate liquid compositions. Note a good fit of results of these calculations with experimental data, especially with regard to NiO for the range 100–200 ppm (*Holzheid et al*., 1994) and 1–2 wt.% (*Campbell et al*., 1979; *Snyder and Carmichael*, 1992). Such calculations were also performed with regard to log f_{O2} and the temperature at known NiO and FeO contents in the melt. These results are shown in Figs. 4c and 4d and demonstrate a high accuracy of estimating the oxygen fugacity (within ±0.1 log f_{O2}). The histograms on the lower graphs give an idea of the accuracy of the temperature calculation.

Topological Peculiarities of the Silicate-Metal Model

Equations (8) for the FeO and NiO solubility with the parameters from Table 1 were combined into a single module. This allowed a model for the equilibrium of Fe-Ni metal with silicate melts of different Fe/Ni ratios to be developed. This subroutine has been incorporated into the basic METEOMOD code (*Ariskin et al.*, 1997), which could be used to study the stability of Fe-Ni liquid and the dependence of the metal composition on the T-f_{O2} parameters and the NiO content in the silicate melt (*Bychkov et al*., 2006). Our numerical experiments simulated the Fe-Ni metal equilibrium conditions in the super-liquidus region of the Saint Severin chondritic melt (Fig. 5), with the NiO contents varying in the range from 10 ppm to 1 wt.%. The calculations were carried out at $-15 \le \log f_{O2} \le -7$. As a result, we established the metal stability field at various NiO contents in the melt (Fig. 5) and revealed the patterns of Fe-Ni metal composition variations in Ni (in metal) – $\log f_{O2}$ coordinates (Fig. 6).

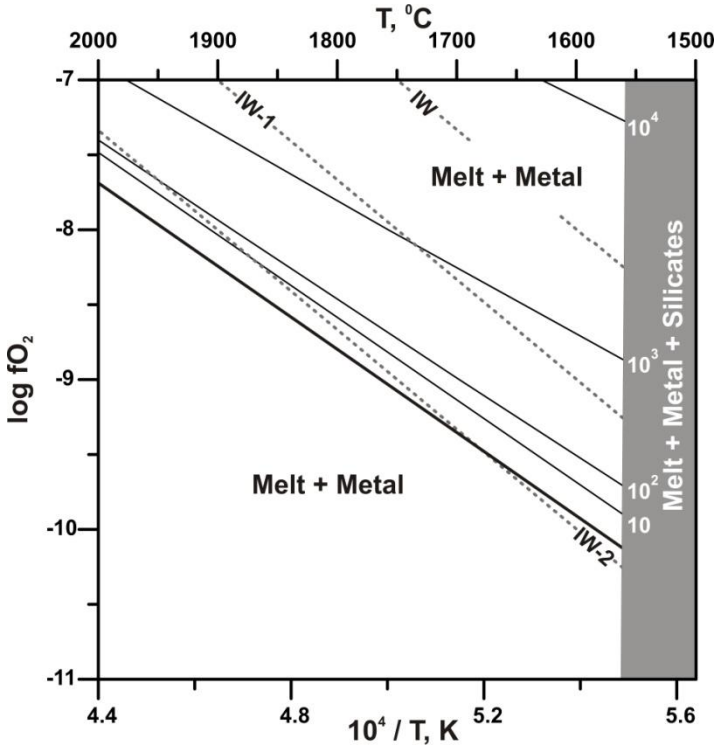

Figure 5. Isopleths of NiO solubility in a super-liquidus chondritic melt in equilibrium with a Fe-Ni liquid (thin solid lines, ppm). The calculations were performed using a revised "nickel" version of the METEOMOD model (*Ariskin et al.*, 1997; *Bychkov et al*., 2006) for a composition corresponding to the Saint Severin LL chondrite (see Fig. 2). The dotted lines correspond to oxygen buffer equilibria parallel to IW. The thicker line represents the isopleth of pure-iron solubility in the same chondritic melt calculated using an empirical equation from Ariskin et al. (1992). The gray background highlights the sub-liquidus region for the given composition at $T < 1560°$ C.

Figure 5 compares the calculated isopleths of NiO solubility in the super-liquidus region of a chondritic melt that correspond to equilibrium with a metallic phase of variable composition. These isopleths with slight variations in slope cross the lines that are parallel to

the IW buffer, and show that increasing the NiO content in the melt leads to an expansion of the Fe-Ni metal stability field towards more oxidizing conditions. At NiO contents of ~ $n \times 10^3$ ppm, the Ni-enriched metal is precipitated at f_{O2} higher than that under the conditions of pure-iron – silicate melt equilibrium by 1.5–2 log units. This situation has a potential for quantifying the relationship between the metal composition and the redox conditions of the medium where the processes of silicate chondrule formation, metal precipitation, and separation could take place.

The metal composition in equilibrium with the chondritic melt under specified redox conditions can be judged from the diagram shown in Fig. 6. This graph was also plotted on the principle of isopleths relating the Ni content in the metal (mol.%) to NiO in the melt and T-f_{O2} parameters. The fact that the results of our calculations point to the existence of a stability field of the relatively Ni-rich alloy – "tenite" (> 10 % Ni if NiO in the melt > 50–100 ppm) and nickel-depleted "kamacite" (< 10 % Ni if NiO in the melt < 50 ppm) - at T > 1560° C is of interest for the subsequent comparison with the metal compositions observed in ordinary chondrites. These melts bear no relation to the decay structures and represent the primary metal reduction products.

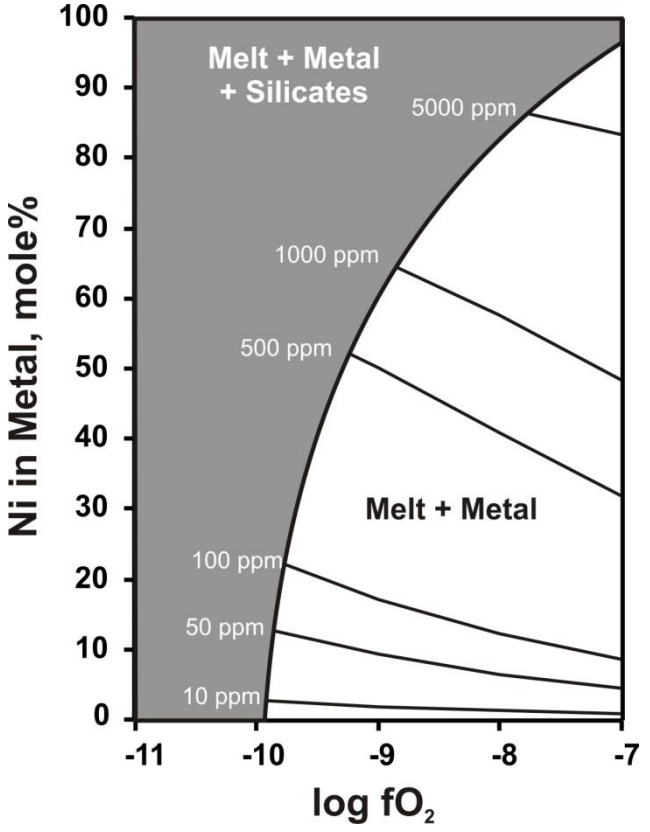

Figure 6. Dependence of the Fe-Ni liquid composition above the silicate liquidus of a chondrite on T–f_{O2} conditions for various NiO contents in the liquid. For the parameters of the calculations, see Fig. 5. The isotherm for the chondrite silicate liquidus T = 1560° C is indicated by the thick line; the isotherms in the super-liquidus region are roughly parallel to this curve. The dotted lines indicate the isopleths of NiO solubility. A specific metal composition corresponds to each point on these isopleths.

The results of these calculations show that the Fe-Ni composition can be an indicator of the evolution conditions for super-liquidus chondritic systems. Thus, despite some imperfections of the METEOMOD program (a more realistic model for the activity of metal components can be developed, the partition coefficients for siderophile elements can be taken into account, etc.), it can be used as a geochemical tool for investigating the thermal reduction processes. The efficiency of applying this model for genetic reconstructions depends upon the possibility of estimating the composition of the protochondritic source that could be subjected to high-temperature heating.

SIMULATION OF THE EVOLUTION OF THE METAL COMPOSITION DURING THERMAL REDUCTION OF GDN CONDENSATES

Table 2. Thermodynamic basis and possibilities of calculations based on various algorithms for simulating the condensation of a solar-composition gas

Possibilities for simulation and specification of input parameters	VAPORS *Ebel and Grossman* (2000)	*Shapkin and Sidorov* (2004)	CWPI *Petaev and Wood* (2005)
Number of chemical elements gas components condensed phases	23 374 125	18* total of ~250 compounds	19 203 488
Thermodynamic database	*Berman* (1988)	DIANIK	*Berman* (1988)
Solid solutions: Ol Opx Cpx Spinel Plag Metal (Fe-Ni) Silicate melt	 + + + + + + +	 no no no no no + no	 + + + + + + no
Equilibrium condensation Fractional condensation	+ no	+ +	+ +
Varying dust/gas ratio in initial system	+	no	+
Nucleation and growth kinetics of metal and *Ol* grains	no	no	+

*The minimal set for the presented models including the components in the H-He-O-P-S-N-C-Si-Al-Fe-Ni-Mn-Cr-Ti-Mg-Ca-Na-K system.

There are several lines of evidence that most silicate chondrules could have been formed through the remelting of previously condensed proto-matter under conditions of its interaction with the GDN gas component (see, e.g., *Libourel et al.*, 2006). It is hypothesized that such melting could have the character of impulsive heating during which the moderately volatile components, including FeO and SiO_2, had no time to evaporate significantly (*Ebel*, 2005). Therefore, it can be assumed that the consequences of high-temperature evaporative differentiation (at least for some siderophile elements) manifested themselves to a larger extent at the stage of melt cooling and primordial chondrule quenching, whereas the initial

composition of these silicate spherules was more likely controlled by the composition of the solar nebular condensate and scales of its thermal reduction (Fig. 2). In attempting to numerically simulate such phenomena, the probable composition of the primordial "solar" condensate should be specified as initial parameters. This is possible by using the present-day GDN condensation models allowing for the variations in *P-T* parameters and proportions of gas and dust.

Differences between the Condensation Models

In recent years, three solar-composition gas condensation models have been discussed in the literature – VAPORS (*Ebel and Grossman,* 2000), CWPI (*Petaev et al.*, 2003; *Petaev and Wood*, 2005), and the program by Shapkin and Sidorov (2004). These models have been developed in the early 1990s and subsequently updated to expand the number of components and the set of variables including kinetic condensation modes. Basic characteristics of these programs are presented in Table 2. All of them were constructed on the principle of minimization of the Gibbs isobaric-isothermal potential $G_{P,T}$ for systems including about 20 most abundant chemical elements (250–600 chemical compounds) at *P-T* parameters corresponding to the hypothetical GDN evolution conditions (the initial condensation temperatures are about 1800 K and the pressure is 10^{-3}–10^{-5} atm). The authors used slightly different procedures of searching for the minimum of $G_{P,T}$, while the Shapkin-Sidorov program (1994–2004) was supplemented by the possibility of controlling the stability of the solution of the thermodynamic equilibrium problem.

The main differences are related to the use of thermodynamic databases and models of solid solutions for the condensed phases to take into account. The VAPORS and CWPI models use an internally consistent database (*Berman,* 1988) for the main petrogenic components (Na_2O-K_2O-CaO-MgO-FeO-Fe_2O_3-Al_2O_3-SiO_2-TiO_2-H_2O-CO_2) corrected for some of the most important reactions and supplemented by an additional information for Ni, Cr, Mn and the gases of the H-He-C-N-O system. A.I Shapkin and Yu.I. Sidorov performed calculations using the DIANIK thermodynamic database developed at the Vernadsky Institute of Geochemistry and Analytical Chemistry, the Russian Academy of Sciences, and adapted for solving cosmochemical problems. As regards the solid solutions, the differences here are fundamental. The authors of the models (*Ebel and Grossman,* 2000; *Petaev et al.,* 2003) managed to include the algorithm (*Ghiorso and Sack,* 1995) proposed to describe the Gibbs free energy in olivine, plagioclase, pyroxene, and spinel solutions (see the review by *Petaev and, Wood*, 2005), while the Shapkin-Sidorov program postulates the possibility of separate condensation for the main end-mineral "rock-forming" phases – forsterite and fayalite, albite and anorthite, diopside and hedenbergite (Table 2). The third important difference is concerned with the possibility of simulating the composition of a high-temperature silicate melt as a condensed phase. Among the listed models, only the VAPORS program gives a subsequent solution of this problem based on a regular solution model for the melt components (for details on the calibration of the MELTS program, see *Ghiorso and Sack*, 1995). This block of calculations is underdeveloped in the CWPI program and is absent in the Shapkin-Sidorov program.

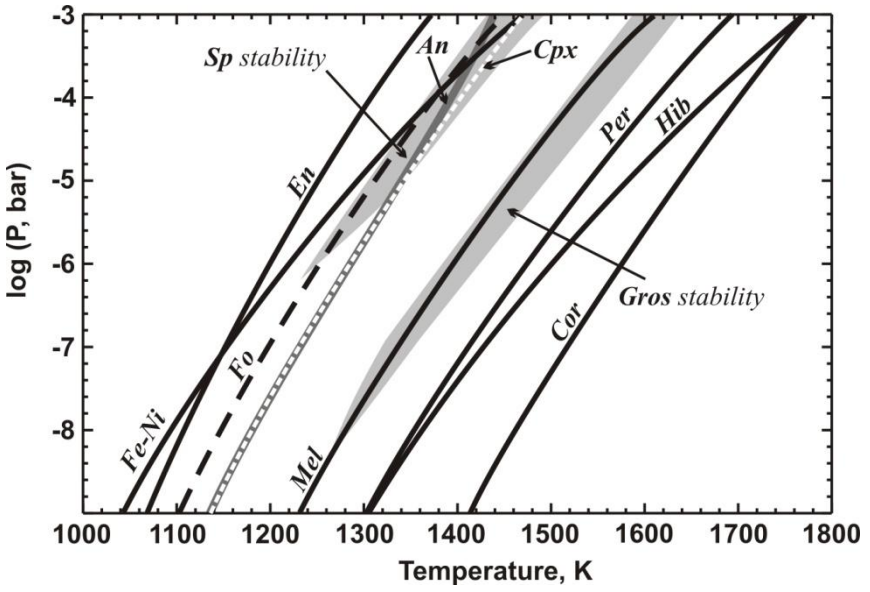

Figure 7**.** The sequence of equilibrium solar-composition gas condensation (*Anders and Grevesse*, 1989) calculated by the CWPI program (*Petaev and Wood*, 2005).

Applying the models disregarding the silicate melt is usually justified by performing calculations at a relatively low gas pressure, 10^{-3}–10^{-4} atm, which leads to the condensation of solid phases, bypassing the stability field of the silicate melt. This is true for an ideal solar gas whose composition corresponds to the solar photosphere (*Anders and Grevesse*, 1989), while its condensation gives rise to virtually entirely reduced mineral assemblages including both forsterite and enstatite (Fig. 7). Variations in the solar-gas composition to simulate more oxidized chondritic materials (which could be the source of silicate chondrules containing a significant amount of FeO) lead to an expansion of the stability field of the silicate melt in the range of moderate and high dust/gas ratios in the original GDN (Fig. 8). In this case, a consistent allowance for the condensation into the liquid phase becomes important (*Alexander*, 2004).

Verification of the proposed algorithms is usually proceeded by comparing the modeled condensation sequences for an ideal solar gas in which the proportions of the assumed dust and gas components correspond to the dust/gas ratio equal to 1 (see below). Table 3 presents some results of such calculations for a solar composition (*Anders and Grevesse*, 1989) at $P = 10^{-3}$ bar. These conditions imply the absence of any liquid condensation products (except for the metal) (*Shapkin and Sidorov*, 2004; *Petaev and Wood*, 2005).

It is easy to see that, on the whole, the VAPORS, CWPI, and Shapkin-Sidorov programs yield consistent results that show a successive replacement of the Ca-Al oxides by rock-forming silicates. However, the absolute temperatures and stability ranges for specific mineral assemblages can differ significantly. The simulation results from Ebel and Grossman (2000) and Petaev and Wood (2005) turn out to be closer than the calculations based on the Shapkin-Sidorov program. These differences include the absence of hibonite and grossite in the model by Shapkin and Sidorov (2004) and revealing of two temperature stages at which the main end-members of the rock-forming oxides and silicates appear – pleonaste (1466° C) and hercynite (610° C), forsterite (1431° C) and fayalite (423° C), anorthite (1418° C) and albite

(819° C). This fundamentally distinguishes the calculations of these authors from other models in which "low-temperature" end-members (hercynite, *Fa*, *Ab*) are present (although in small quantities) in the condensed solid solutions earlier by 600–1000° C. This discrepancy cannot but affect the proportions of the main phases of condensed systems and (what is especially important) the mineral compositions. In particular, the "average" mg# of olivine in the model condensate (*Shapkin and Sidorov*, 2004) was estimated simply by dividing the calculated amount of *Fo* in the system into the sum of the molecular amounts of *Fo* and *Fa* as independent phases. In the models by Ebel and Grossman (2000 and Petaev and Wood (2005), the *Fo* content in olivine is calculated for a solid olivine solution.

We focus attention on this question, because therein lies the cause of yet another important mineralogical difference in the composition of the calculated condensates of an ideal solar gas. The calculations by Ebel and Grossman (2000) and Petaev and Wood (2005) in the case of equilibrium condensation give a *Fa* content in olivine of no more than 0.1 mol.%, whereas the Shapkin-Sidorov program yields up to 20–25 % *Fa* in "averaged" olivine from the bulk condensed material. Apparently for this reason, these authors did not face the problem of an extremely high degree of reduction of the condensation products of an ideal solar gas (*Anders and Grevesse,* 1989) and the necessity of varying the GDN composition to choose the conditions corresponding to more oxidized silicate chondrules that contain significant amounts of FeO (*Fa* in olivine).

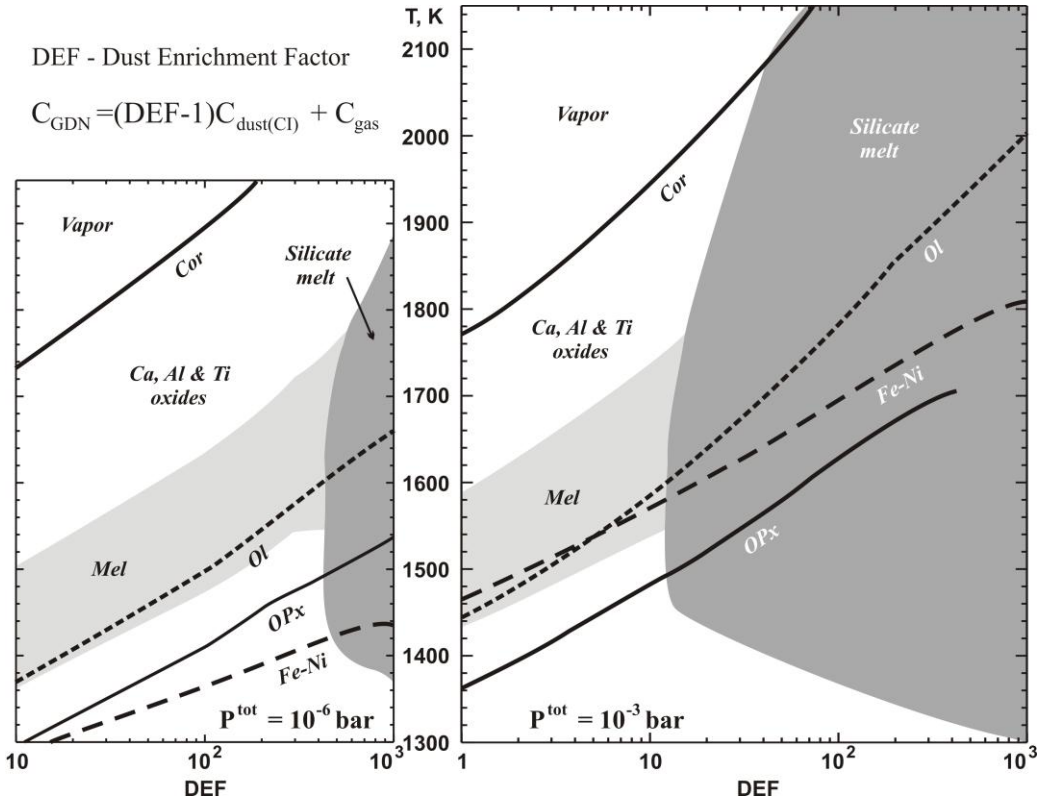

Figure 8. The melt stability fields as a function of the pressure and dust/gas ratio in the nebula. Based on the review by Petaev and Wood (2005) with modifications.

The Effect of the Dust/Gas Ratio in the Solar Nebula

The solution to the problem of a relatively high oxidation of the GDN regions where the proto-source of silicate chondrules was formed is found in spatial variations of the solar-gas composition (*Ebel and Grossman*, 2000; *Petaev et al.*, 2003; *Alexander*, 2004). In this case, it is implied that the constancy of the bulk composition of the solar system is consistent with the fact that the GDN composition varied both laterally and vertically at different distances from the disk center (*Dorofeeva and Makalkin*, 2004; *Zanda et al*., 2006). The physical causes of these variations can be different, but experts on the simulation of condensation processes use the dust enrichment factor (DEF) or the dust/gas ratios in the initial system as a measure or degree of deviation from an ideal solar gas. In particular, Ebel and Grossman (2000) used the mixing of two components – an ideal solar gas and dust corresponding to the average composition of carbonaceous CI chondrites (Table 4) – to calculate the composition of dust-condensate-enriched systems.

Table 3. The sequences of condensation of mineral phases from a solar-composition gas (*Anders and Grevesse,* 1989) at $P = 10^{-3}$ bar

Mineral phase	VAPORS *Ebel and Grossman* (2000)		*Shapkin and Sidorov* (2004)		CWPI *Petaev and Wood* (2005)	
Temperature range, K (appearance – *disappearance of phases*)						
Corundum, Al_2O_3	1770	1726	1771	1466	1775	1751
Hibonite, $CaAl_{12}O_{19}$	1728	1686	–	–	1770	1495
Grossite, $CaAl_4O_7$	1698	1594	–	–	1656	1606
Perovskite, $CaTiO_3$	1680	1458	1692	1412	1692	1465
$CaAl_2O_4$	1624	1568	–	–	–	–
Melilite (ss)	1580	1434	1640 [*]	1440	1608	1450
Grossite, $CaAl_4O_7$	1568	1502	–	–	–	–
Hibonite, $CaAl_{12}O_{19}$	1502	1488	–	–	–	–
Spinel (ss)	1488	1400	1466 [2*]	1418	1495	1431
Metal (ss)	1462		1459 [3*]		1472	
Clinopyroxene (ss)	1458		1440 [4*]	398	1466	
Olivine (ss)	1444		1431 [5*]		1449	
Plagioclase (ss)	1406	1318	1418 [6*]	610	1460	
Ti_3O_5	1368	1342	1412	1253	1380	
Orthopyroxene (ss)	1366		1381 [7*]		1372	
Ti_4O_7	–		–	–	1350	
Cordierite, $Mg_2Al_4Si_5O_{18}$	1330		–	–	–	
Cr spinel (ss)	1230		–	–	1170	
Albite ($NaAlSi_3O_8$)			819	407		
Hercynite ($FeAl_2O_4$)			610			
Fayalite (Fe_2SiO_4)			423			

Notes. [*] Helenite ($Ca_2Al_2SiO_7$), [2*] pleonaste ($MgAl_2O_4$), [3*] metallic iron, [4*] diopside ($CaMgSi_2O_6$), [5*] forsterite (Mg_2SiO_4), [6*] anorthite ($CaAl_2Si_2O_8$), [7*] enstatite ($MgSiO_3$).

Table 4. Relative atomic abundances of elements in an ideal solar-composition gas, the CI component (normalized to 10^6 Si atoms), and dust-enriched model compositions relative to the solar composition

	AG89 (=I)	Dust (=CI)	«100 × CI»	«1000 × CI»	II	III
H	2.79×10^{10}	5.28×10^{6}	2.84×10^{10}	3.32×10^{10}	**7.32×10^{6}**	**2.83×10^{6}**
He	2.72×10^{9}		2.72×10^{9}	2.72×10^{9}	2.72×10^{5}	2.72×10^{5}
C	1.01×10^{7}	7.56×10^{5}	8.50×10^{7}	7.65×10^{8}	**6.00×10^{6}**	**1.01×10^{4}**
N	3.13×10^{6}	5.98×10^{4}	9.05×10^{6}	6.28×10^{7}	3.13×10^{2}	3.13×10^{3}
O	2.38×10^{7}	7.63×10^{6}	7.80×10^{8}	7.65×10^{9}	**4.92×10^{7}**	**3.71×10^{7}**
F	8.43×10^{2}	8.43×10^{2}	8.43×10^{4}	8.43×10^{5}		
Ne	3.44×10^{6}		3.44×10^{6}	3.44×10^{6}		
Na	5.74×10^{4}	5.74×10^{4}	5.74×10^{6}	5.74×10^{7}	5.74×10^{4}	5.74×10^{4}
Mg	1.07×10^{6}	1.07×10^{6}	1.07×10^{8}	1.07×10^{9}	1.07×10^{6}	1.07×10^{6}
Al	8.49×10^{4}	8.49×10^{4}	8.49×10^{6}	8.49×10^{7}	8.49×10^{4}	8.49×10^{4}
Si	1.00×10^{6}	1.00×10^{6}	1.00×10^{8}	1.00×10^{9}	1.00×10^{6}	1.00×10^{6}
P	1.04×10^{4}	1.04×10^{4}	1.04×10^{6}	1.04×10^{7}	1.04×10^{4}	1.04×10^{4}
S	5.15×10^{5}	5.15×10^{5}	5.15×10^{7}	5.15×10^{8}	5.15×10^{5}	5.15×10^{5}
Cl	5.24×10^{3}	5.24×10^{3}	5.24×10^{5}	5.24×10^{6}	5.24×10^{3}	5.24×10^{3}
Ar	1.01×10^{5}		1.01×10^{5}	1.01×10^{5}		
K	3.77×10^{3}	3.77×10^{3}	3.77×10^{5}	3.77×10^{6}	3.77×10^{3}	3.77×10^{3}
Ca	6.11×10^{4}	6.11×10^{4}	6.11×10^{6}	6.11×10^{7}	6.11×10^{4}	6.11×10^{4}
Ti	2.40×10^{3}	2.40×10^{3}	2.40×10^{5}	2.40×10^{6}	2.40×10^{3}	2.40×10^{3}
Cr	1.35×10^{4}	1.35×10^{4}	1.35×10^{6}	1.35×10^{7}	1.35×10^{4}	1.35×10^{4}
Mn	9.55×10^{3}	9.55×10^{3}	9.55×10^{5}	9.55×10^{6}	9.55×10^{3}	9.55×10^{3}
Fe	9.00×10^{5}	9.00×10^{5}	9.00×10^{7}	9.00×10^{8}	9.00×10^{5}	9.00×10^{5}
Co	2.25×10^{3}	2.25×10^{3}	2.25×10^{5}	2.25×10^{6}	2.25×10^{3}	2.25×10^{3}
Ni	4.93×10^{4}	4.93×10^{4}	4.93×10^{6}	4.93×10^{7}	4.93×10^{4}	4.93×10^{4}

Note. AG89 – the solar composition from Anders and Grevesse (1989) that we used as composition I (Tables 5 and 6). The "100 × CI" and "1000 × CI" compositions represent the **GDN** composition calculations using the technique by Ebel and Grossman (2000): $C_{\mathbf{GDN}} = (DEF - 1)C_{\text{dust}} + C_{\text{AG89}}$. Compositions II and III represent the calculations with various proportions of conditionally solar components using the technique by Wood and Hashimoto (1993) and Petaev et al. (2003): II – dust/organics/gas/ice proportions = 1/1/0.0001/0.0001; III – dust/organics/gas/ice proportions = 1/0.001/0.0001/0.001.

Figure 9 presents the results of the calculations based on the VAPORS program, which simulate the change in oxygen fugacity (log f_{O2}) during the condensation of systems with different DEFs (Table 4). These data show that an increase in DEF causes the oxygen potential in an equilibrium gas system to increase. This is a result of the redistribution of O, H, and C species between the silicates and the most important solar-gas components, including H_2, CO, H_2O, and CO_2. The oxygen fugacity in the gas medium increases through the separation of "reduced" (H_2, CO) and "oxidized" (H_2O, CO_2) components. The degree of such separation increases as the dust component is accumulated in the system: at $DEF \sim 500$–1000, the redox conditions of the condensing system turn out to be lower than the iron-wüstite (IW) buffer by 1.5–2 log units. Under these conditions, much of the iron enters into the silicate matrix in the form of FeO.

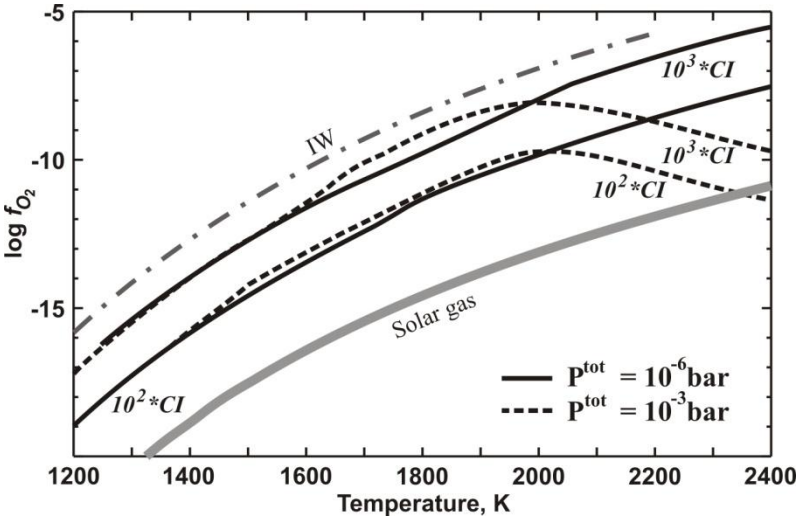

Figure 9. Oxygen fugacity versus temperature of solar-gas equilibrium with the **GDN** condensates. The results of the calculations based on the VAPORS program at two pressures for two solar compositions differing by *DEF* (100× и 1000×) from Ebel and Grossman (2000).

The approach presented above (Table 4, Fig. 9) implies that the compositional component of the dust is initially present in the solar gas whose composition can be described as a mixture of two end-components – an ideal gas (including H + He + Ne + Ar) and CI dust (given the solar element abundances). There are possibilities for expressing the GDN composition variations using the proportions (ratios) of other "conditionally solar" components. The tradition of such a description originates from the paper by Wood and Hashimoto (1993) and includes the consideration of four main components of the solar material – gas (H + He), ice (H, C, N, O), organics (H, C, O), and dust. The CWPI program admits variations in ratios for these end-components, which lead to a change in GDN composition and the corresponding redox conditions. Thus, the integral dust component in the CWPI model is represented as a mixture of ice, organics, and residual dust in proportions providing the solar element abundances.

Therein lies the difference between the composition of the non-gas component from Petaev et al. (2003) and the CI component used by Ebel and Grossman (2000). These differences are most pronounced for C, N, and O, which show an enrichment of the residual dust calculated in this way relative to the CI composition approximately by a factor of 13, 52, and 3, respectively (*Petaev and Wood*, 2005). For this reason, lower dust/gas rations (usually in the range 0.1–50) than those in the VAPORS program (100–1000) are used to estimate the dust-enriched GDN compositions in the CWPI model. These differences are not fundamental, because, irrespective of the *DEF* or the dust/gas ratio, achieving the same degree of oxidation of the condensing system requires close bulk compositions for the original GDN. Both models allow these compositional characteristics to be varied over a wide range, given that an increase in the dust/gas ratio in the initial system shifts the total silicate melt stability pressure to the region of lower values (Fig. 8).

A certain advantage of the VAPORS program over the CWPI code is the possibility of calculating the composition of the condensed silicate liquid. However, this plus is of no crucial importance, given that such calculations are based on the MELTS model for the activity of melt

components, whose reality even in the calibration range of temperatures (below the liquidus of basalt- peridotite systems) is questioned by the authors themselves (*Ghiorso et al*., 2002). The CWPI program appears attractive with regard to condensation calculations under conditions of partial or total isolation of the condensed material (Table 2). For the first numerical experiments on the thermal reduction of GDN condensates, we chose the CWPI model, whose code was kindly provided by M.I. Petaev.

Table 5. The mineral composition of the model condensates calculated using the CWPI program (Petaev et al., 2003; Petaev and Wood, 2005)

Wt. %	I		II		III		
	1000 K	800 K	1000 K	800 K	1200 K	900 K	800 K
Ol	25.65	15.4	4.74	6.02	46.44	41.00	43.08
Metal	32.22	31.34	1.27	17.60	24.6	7.70	7.04
Opx	31.77	42.00	–	29.53	12.60	12.7	10.88
Cpx	2.6	2.84	–		2.83	3.02	3.37
Plagioclase	7.45	6.69	–	7.93	10.31	9.71	10.10
Shreibersite	–	0.87	–	0.67	–	–	–
Periclase	–	–	9.04	–	–	–	–
Spinel	–	0.67	3.77	–	–	0.72	0.78
Sulfide (cub. mod.)	–	–	15.7	.59	–	–	–
Fe–Ni sulfide	–	–	–	9.12	–	23.27	23.31
CaS	–	–	2.75	1.50	–	–	–
Graphite			13.61	21.33	–	–	–
Silicides (Me/Si)	–	–	48.48	–	–	–	–
β– cristobalite	–	–	–	–	0.71	–	–
Whitlockite	–	–	–	–	–	–	0.85
Other phases	≤ 0.31	≤ 0.11	≤ 0.59	≤ 0.71	≤ 2.45	≤ 1.82	≤ 0.59

Notes: I–III – see the model **GDN** compositions in Table 4. Only the phases whose amount in the model condensates is at least 0.5 wt. % are listed.

Evolution of the Melt and Metal Compositions during Thermal Reduction

The model calculations have been separated in two stages. Initially, the compositions of the "solar" condensates were estimated using the CWPI program for various condensation temperatures and dust/gas ratios; subsequently, the compositions of these model condensates (recalculated on oxide basis) were used in the METEOMOD program to simulate their heating and reduction above the olivine liquidus temperatures.

The condensation calculations included the specification of *P-T* parameters in the solar nebula for the region of probable chondrule formation (dust/gas ratios) and the bulk composition of the condensing system. The pressure in the nebula was estimated by various authors to be within the range 10^{-4}–10^{-3} atm, while its variations in this range do not affect strongly the order of condensation, except for the olivine-metal reversion (Fig. 7). In our calculations, we assume $P = 10^{-4}$ atm (see, e.g., *Dorofeeva and Makalkin*, 2004). The key point is to specify the initial GDN composition. Actually, the "ideal solar composition" implies using one of the two popular models – those of Anders and Grevesse (1989) and Lodders (2003).

However, this most primitive (averaged over the nebula) composition of the solar material can be varied through the proportions of dust and gas as the conditionally solar components. Using the CWPI program, we calculated and examined three variants of the protochondritic source based on the data from Anders and Grevesse (1989): (I) a canonical solar composition (AG89) with undisturbed proportions of the conditionally solar components and two highly dust-enriched compositions – with relatively high (II, dust/organics/gas/ice = 1/1/0.0001/0.0001) and reduced (III, dust/organics/gas/ice = 1/0.001/0.0001/0.001) carbon contents. The gas content in the compositions II and III was reduced by four orders of magnitude (Table 4). The condensation temperatures for these compositions were varied in the range 800–1200 K (Table 5). At fixed parameters of our calculations, the volatile components (CO, CO_2, H_2O, sulfur, nitrogen, and alkali metal compounds) are concentrated mainly in the gas phase, while the average mineral composition of the calculated condensates may be considered as a model of the protosource of silicate chondrules and metal differently depleted in volatiles.

Table 6. The chemical composition of the model condensates and a metal-poor LL chondrite assuming complete iron and nickel oxidation

Wt. %	I		II		III			STS
	1000 K	800 K	1000 K	800 K	1200 K	900 K	800 K	
SiO_2	31.67	32.99	33.77	32.69	32.77	32.66	32.66	40.78
TiO_2	0.1	0.11	0.11	0.10	0.10	0.10	0.10	0.11
Al_2O_3	.58	2.38	2.46	2.35	2.36	2.35	2.35	2.38
"FeO"	35.38	35.51	35.75	35.18	35.26	35.16	35.13	26.01
MnO	0.01	0.01	0.35	0.37	0.36	0.37	0.37	0.32
MgO	25.43	23.77	21.63	23.56	23.61	23.53	23.53	25.31
CaO	2.05	1.88	1.95	1.86	1.87	1.86	1.86	1.93
Na_2O	0.00	0.02	0.00	0.88	0.79	0.95	0.96	1.00
K_2O	0.00	0.00	0.00	0.04	0.03	0.05	0.08	-
P_2O_5	0.13	0.39	0.31	0.40	0.27	0.40	0.40	0.22
Cr_2O_3	0.47	0.56	0.58	0.56	0.56	0.56	0.56	0.58
"NiO"	2.15	2.02	2.09	2.00	2.00	2.00	2.00	1.35
T_{Ol},°C	1595	1587	1568	1567	1558	1558	1558	1552

Notes: I–III – see the model **GDN** compositions and their condensation products in Table 4. The contents of the iron and nickel oxides were calculated based on the composition of the model condensates (Table 5) as "FeO" = FeO + Fe and "NiO" = NiO + Ni. The STS composition corresponds to the bulk composition of the Saint Severin LL chondrite from Jurewicz et. (1995). The silicate liquidus temperature was estimated by means of the Ol thermometers used in the METEOMOD program (*Ariskin et al*., 1997): the NiO content in the melts was disregarded in this case.

Comparing the mineral characteristics of these condensation products is of interest (Table 5). For the "solar composition" I, they are represented by a mixture of metal (about a third) and silicates. For the carbon-enriched composition II, we point out a sharply reduced character of the system containing graphite and metal silicides. The condensation products of the most dust-enriched composition III are dominated by olivine (41–46 wt.%) and a metal-sulfide mixture (collectively 25–30 %) at fairly stable proportions of *Opx*, *Cpx*, and plagioclase. We consider such mineral compositions as the most probable model systems for the

protochondritic source. The results of recalculating these mineral compositions (Table 5) to the mass fractions of 12 "petrogenic" oxides are presented in Table 6. The constancy of these "petrochemical" characteristics is not surprising – basically, they represent the virtual oxidation product of the silicate component of the solar material. For comparison, the last column in Table 6 gives the composition of the Saint Severin LL chondrite, which is one of the most primitive ordinary chondrites (*Jurewicz et*., 1995). Obviously, the composition of this LL chondrite bears evidence for the early removal of ~12 % of the metallic phase with subchondritic proportions of Fe and Ni from the solar composition.

For the further calculations and comparisons, we choose a condensation product of the composition III at 1200 K (927° C) and a system corresponding to the Saint Severin chondrite (Table 6). Both systems were used as an approximation of the bulk composition of protochondritic materials in our calculations based on the "nickel" version of the METEOMOD program.

The simulation of thermal reduction begins with the calculation of two temperatures corresponding to olivine-melt (T_{Ol}) and metal-melt (T_M) equilibrium at arbitrary log f_{O2}. Since the regime of thermal reduction is to take place in the super-liquidus region of the initial system, it is important to choose such an oxygen fugacity that the difference between the metal equilibrium temperature and the olivine liquidus $T_M - T_{Ol} > \varepsilon_T$ (where $\varepsilon_T > 0$ is of the order of the first degrees). Under this condition and at constant log f_{O2}, the calculations start in the regime of thermal reduction when the temperature is to increase as a metal of variable composition precipitates (see trajectory II in Fig. 2b). We choose log $f_{O2} = -6.70$ ($T_{Ol} = 1558°$ C) for the composition III (1200 K) in Table 6 and log $f_{O2} = -7.00$ ($T_{Ol} = 1552°$ C) for STS. These initial parameters correspond to the redox conditions ~ IW + 1; starting from a temperature of ~1740° C, both systems evolve at more reducing conditions than those for the iron-würstite buffer. This is in good agreement with the data on direct oxygen fugacity measurements in various types of ordinary chondrites (*Brett and Sato*, 1984; *McSween and Labotka*, 1993), see Schaefer and Fegley (2007). As a result of these incremental calculations with a step of 1 wt.%, we obtain a set of compositions for chondrule-forming liquids that are in equilibrium at different temperatures with a certain amount of Fe-Ni metal.

Figure 10 displays the calculated co-variations in residual melt composition, equilibrium composition, and the amount of reduced metal for the chosen initial compositions during the thermal reduction. The estimates of the average composition for three main types of ordinary chondrites from Schaefer and Fegley (2007) are given for comparison. Both modeled systems cover a wide range of temperatures (~1560–2200^o C) and degrees of reduction of the initial condensates whose melting products change regularly with the precipitated metal proportion. For the main oxide components, the calculated trajectories display monotonous trends of evolution due to the depletion of FeO in the melt and complementary accumulation of the remaining components. This is an obvious result. Note only that if ordinary chondrites are assumed to be a mixture of thermal reduction products from the melt (chondrules plus metal) and a primitive condensed material (matrix), then compositions similar to those of the Saint Severin chondrite approximate satisfactorily the composition of this initial material.

Also, the model relationships between the metal proportion and composition are interesting (Fig. 10). In both cases, a high NiO content and an enhanced oxygen fugacity (~IW+1) initially leads to the precipitation of a Ni-rich phase with a Ni content of about 90 %. However, even at 5 % of the metal reduction, we observe a Ni content of about 30 %,

which is monotonously decreased towards the "solar" Ni/Fe ratio (Table. 6). This is a nontrivial result based on the thermodynamic model for the Fe-Ni alloy (*Tomiska and Neckel,* 1985), the experimental data on the Fe and Ni solubility in silicate systems, and the T-f_{O2} regime of the thermal reduction. The genetic significance of the cosmochemical reconstructions is given below.

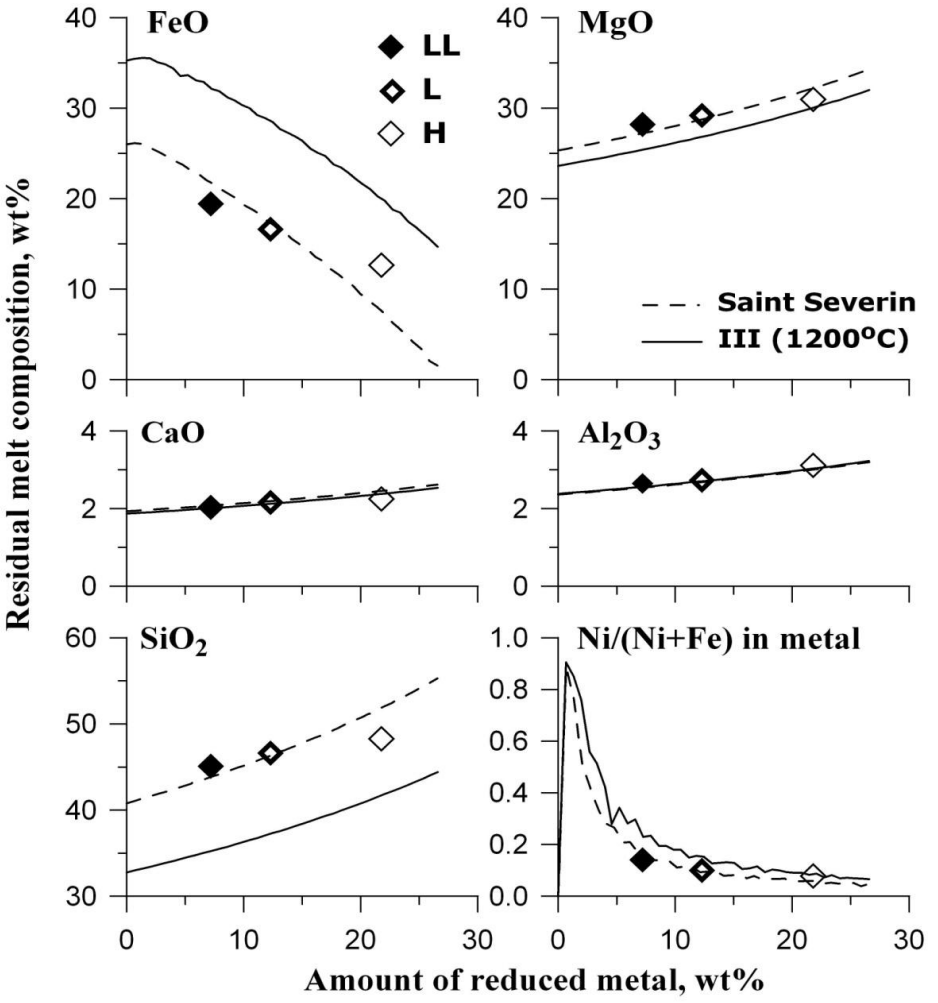

Figure 10. Results of calculations simulating thermal reduction of Fe-Mi metal from the silicate melts consistent with possible protochondritic sources. The initial materials included a model condensate of solar-composition gas (composition III at 1200 K) and a source corresponding to the primitive Saint Severin LL chondrite (STS), see Tables 4–6. The calculations were performed at temperatures above the silicate liquidus and P = 1 atm based on a revised version of the METEOMOD program (2006–2008): the reduction step is 0.5 wt.%, log f_{O2} = const (-6.70 for III-1200 and -7.00 for STS). The average compositions of ordinary LL, L, and H chondrites were taken from Schaefer and Fegley (2007). The temperature range of the reduced melts is ~1560–2200° C.

DISCUSSION

Experiments on the melting of possible protochondritic materials (*Cohen et al*., 2004; *Cohen and Hewins*, 2004), numerical simulations of the condensation processes in the nebula (see above), and local chemical analyses for silicate chondrules and metal grains in the most primitive chondrites have allowed one to approach the estimation of GDN parameters in chondrule formation regions and to identify the geochemical contradictions when formulating various hypothesis of their formation (*Connoly et al*., 2001; *Campbell et al.*, 2005). About ten genetic models have been proposed to describe the origin of metal. These include:

[1] the condensation from the solar nebula into the solid (*Grossman and Wasson*, 1985; *Jones*, 1994; *Campbell et al.*, 2005) or liquid (*Ebel and Grossman*, 2000; *Varela et al.*, 2006) phases;
[2] the FeO reduction from the protochondritic melt through the reactions with carbon (*Hanon et al*., 1998; *Connoly et al*., 2001) and hydrogen (*Sears et al*., 1996; *Cohen and Hewis*, 2004) or through thermal reduction (*Ariskin et al.*, 1997, 2006);
[3] the metal precipitation as a result of iron sulfide desulfurization (see, e.g., *Zanda et al*., 1994);
[4] the Fe^0 recondensation through the material precipitated previously during the evaporation of chondrule-forming melts (for CR2 chondrites, see *Connoly et al*., 2001);
[5] the impact on the protochondritic source (*Kallemeyn et al*., 2001; *Campbell et al*., 2002);
[6] the reduction from silicates during metamorphic processes on the parent body of chondrites (*Lee et al*., 2002);
[7] the presence of a pre-existed metal.

The large-scale chondrule formation and metal formation processes include the mechanisms of GDN condensation and the precipitation of Fe-Ni alloys from high-temperature protochondritic melts. The primitive (solar) Co/Ni ratios in the condensed material that were predicted by the first calculations of solar-composition gas condensation (*Grossman and Olsen*, 1974) and the weakly fractionated spectra of the siderophile elements dominating in metal grains from typomorphic samples of ordinary chondrites (*Krot et al*., 2003; *Campbell et al.*, 2005) are the main arguments for the condensational origin of the metal in chondrites. The studies of the distribution of siderophile elements for carbonaceous chondrites of the "CR family", which are characterized by an insignificant degree of metamorphism and a high content of the metallic phase (*Kong and Palme*, 1999; *Connoly et al*., 2001; *Campbell et al.*, 2002; *Campbell and Humayun*, 2003, 2004), have attracted attention in recent years. This group includes Renazzo-type chondrites (CR proper, *Weisberg et al*., 1993), CH (*Bischoff et al*., 1993), and bencubbinites (the subtypes CB_a and CB_b, *Weisberg et al*., 2001). These objects are interesting in that the siderophile elements in them not only exhibit insignificant deviations of the geochemical ratios from the primitive (solar) ones but, in several cases, also show complementarity of the chemical composition of silicate chondrules and the amount of metallic phase (*Connoly et al*., 2001). Data on the metal composition in bencubbinites and the Grossvenor Mountains 95551 chondrite strongly suggest that the full spectrum of their geochemical characteristics cannot be explained in

terms of the model of condensation from the gas phase into the solid one (*Campbell et al.*, 2002; *Campbell and Humayun*, 2003).

The models taking into account the important role of high-temperature chondrule-forming melts not only operate with the geochemical ratios but also allow for the physical constraints based on the structural observations and the use of partition coefficients in the silicate-metal system. These constraints include several fundamental observations (*Connoly et al*., 2001):

[1] the round shapes and magmatic structures of most chondrules indicate that they crystallized from molten droplets;
[2] the metal in silicate chondrites is also represented by isometric spherules or fills interstices between the boundaries of silicate grains – this is evidence for the presence of an immiscible metallic melt;
[3] the presence of a liquid Fe-Ni alloy (≤ 10 % Ni in the metal) allows constraints to be imposed on the minimum temperature of the heterogeneous chondrule-forming system, about 1510° C (*Swartzendruber et al.*, 1991);
[4] the results of experiments on the melting of chondrules and calculations of their liquidus temperatures pointing to a range ~1550–1800° C (see, e.g., *Cohen et al*., 2000) are also consistent with this estimate.

The fact that the silicate chondrules and the metal inside the chondrules existed in the form of immiscible melts suggests that efficient partitioning of siderophile elements is inevitable. The dependence of the bulk composition of silicate chondrules on the amount of metal present in them can be a geochemical signature of such fractionation. Such estimations for Renazzo-type (CR2) chondrites show that metal-depleted chondrules turned out to be depleted in siderophile elements, irrespective of their volatility (*Connoly et al*., 2001). The problem of stable "nonfractionated" (solar) Os/Ir, Ni/Fe, Co/Ni, Pt/Fe, and other ratios, which are typical of the central parts of most metal grains (*Campbell et al*., 2005), remains. The experimental data obtained at $P = 1$ atm under low oxygen fugacity conditions ($\log f_{O2} \le -10$) indicate that the metal-silicate partition coefficients in high-temperature basaltic and chondritic systems are $D_{M\text{-Sil}} \sim 10^2$–$10^3$ for moderately siderophile elements (Co, Ni) and reach $D_{M\text{-Sil}} \sim 10^4$ for highly siderophile platinoids (*Schmitt et al.*, 1989; *Walter et al.*, 2000; *Righter*, 2003). High contents of siderophile elements in the metal and a fractionated spectrum of partitioning relative to the "initial" iron content in CI chondrites were predicted on the basis of these data. The dominance of metal grains with a nickel content of about 5–5.5 % (Fe/Ni ~ 18) in chondrites seems to be in conflict with these estimates; see the "solar" composition in Table 4.

Meanwhile, an elementary analysis of the partitioning laws in the metal-silicate system gives an obvious explanation for this contradiction. Consider 1 mole of a silicate system containing some amount of Fe and Ni oxides ($[SiO_2] + \ldots + [FeO] + + [NiO] + \ldots = 1$ mole). Assume that this system has been separated into f moles of the metal ($X_{Ni} + X_{Fe} = 1$) and $(1 - f)$ moles of the silicate melt with certain contents X_{FeO} and X_{NiO}. The siderophile element balance equations for this heterogeneous system are

$$[FeO] = (1 - f)\, X_{FeO} + f\, X_{Fe}, \qquad (9a)$$

$$[\mathrm{NiO}] = (1 - f)\, X_{\mathrm{NiO}} + f\, X_{\mathrm{Ni}}. \quad (9b)$$

In the case of high Ni partition coefficients between the metal and the melt ($D_{Ni} \sim 10^3 >> 0$), it can be assumed that almost all of the nickel is concentrated in the metal, i.e., $(1 - f)X_{\mathrm{NiO}} \sim 0$:

$$1 / X_{\mathrm{Ni}} = f / [\mathrm{NiO}]. \quad (10)$$

Given the stoichiometry, let us express the Fe/Ni ratio in the metal as

$$X_{\mathrm{Ni}} / X_{\mathrm{Fe}} = X_{\mathrm{Ni}} / (1 - X_{\mathrm{Ni}}) = 1 / (1 / X_{\mathrm{Ni}} - 1). \quad (11)$$

Substituting (10) into (11) gives the predicted composition of the metallic phase

$$X_{\mathrm{Ni}} / X_{\mathrm{Fe}} = X_{\mathrm{Ni}} / (1 - X_{\mathrm{Ni}}) = 1 / (f / [\mathrm{NiO}] - 1). \quad (12)$$

Equation (12) shows that since nickel is highly siderophilic, the equilibrium metal composition does not depend on the initial iron content in the system but is determined by the amount of reduced phase f and the NiO content in the source. The total iron content serves as the constraint $f \leq [\mathrm{FeO}]$, which in the upper limit corresponds to complete metal reduction $f_{\max} = [\mathrm{FeO}]$. If we take [FeO] ~ 0.352 and [NiO] ~ 0.02 (Table 6) for the primitive, but oxidized solar condensate, then at the maximum degree of reduction we obtain a metal composition with Ni/Fe ~ 0.06 that is close to the chondritic one. This approximate calculation shows that the observed primitive composition of the metallic grains in chondrites is not only consistent with the concept of reduction from a melt but is a direct consequence of the partitioning in the metal-silicate system at a high degree of proceeding the reaction (2). Obviously, this logic is applicable to other highly siderophile elements whose partitioning can also be described by Eqs. (10)–(12). Thus, the clear correlations and the consistency of the cosmochemical ratios in the metal for nonvolatile and moderately volatile siderophile elements can be explained – this is also a consequence of the extremely high degree of reduction of silicate chondrules. The available estimates of olivine compositions in silicate chondrules, which usually point to forsterite containing no more than 1–2 mol.% *Fa* (*Krot et al*., 2003), serve as an indirect confirmation of this regularity. The data on the compositions of silicate minerals in CR chondrites, where the Ni content in individual metal grains reaches 8–12 % (*Connoly et al*., 2001; *Campbell and Humayun*, 2003), seem extremely important in this connection. Such a composition may be considered as evidence for incomplete metal reduction from the initial melts and the expected more ferrous composition for the corresponding silicate matrix.

We believe that the proposed concept of thermal reduction of Fe-Ni metal offers new ways of solving traditional problems of meteoritics. The experimental data on the melting of ultramafic materials, thermodynamic analysis of the transitional metal reduction conditions, and the models presented above (Fig. 10) indicate that the formation of metal from a silicate molten material is inevitable in virtually any high-energy process in which the temperature exceeds 1500–2000° C. If this conclusion is applied to the formation of primordial silicate chondrules and metallic spherules in the solar nebula, then the following mechanisms are proposed as realistic physical ones: (1) the action of shock waves on the GDN through a supernova

explosion, (2) ablation and/or aerodynamic heating during protoplanetary disk accretion, (3) lightning discharges in the gas-dust cloud, and (4) gasdynamic impact heating during the collisions of gas streams with different densities and temperatures (*Rubin*, 2000). Such processes may be considered as "impulsive" ones in the sense that their time scale does not exceed fractions of a second or the first minutes. It can be noted that for almost complete metal reduction in King's experiments (*King*, 1983), it was sufficient to heat the source from 1400 to 3000° C in one minute. The chronology of the chondrule formation events in high-temperature processes corresponds to a time interval of ~2 Myr – from the formation of CAIs to the appearance of the first planetesimals (*Trieloff and Palme*, 2006). The thermal metal reduction mechanism at the earliest evolutionary stages of the gas-dust nebula considered is consistent with the W-Hf systematics of meteoritic matter, according to which the iron meteorites and the chondrite metal have low values of $\varepsilon(^{182}W)$, from –4 to –3, at Hf/W ≈ 0 (*Jones and Palme*, 2000).

CONCLUSION

We provided experimental evidence (*Barmina et al.*, 1974; *King*, 1982, 1983; *Yakovlev et al*., 1985, 1987, 2003), thermodynamic arguments (*Ariskin et al.*, 1997), and numeric models (*Ariskin et al*., 2006; *Yakovlev et al*., 2008) arguing for the wide range of temperatures when the protochondritic systems were heated above the olivine liquidus is the main cause of the differences in the degree of metal reduction and the conjugate compositional evolution of silicate chondrules (Figs. 2 and 3). Thus, the formation of complementary chondrules and metal, as the main components of ordinary chondrites, may be considered in the context of rapid differentiation in which the scales of the phase separation for primordial materials can be directly related to the degree (efficiency) of the temperature jump. Our numerical simulations of thermal reduction for chondritic and protochondritic melts were performed assuming log f_{O2} = const, which implies the absence of significant variations in the composition of the gas medium under impulsive heating conditions. However, this scheme does not necessarily suggest a constant oxygen fugacity. Variations in log f_{O2} under the conditions of the protosolar nebula that correspond to a gentler slope of the dependence of log f_{O2} on the reciprocal temperature than that for the Fe-FeO buffer (Fig. 2) are also possible for the manifestation of the thermal reduction effects. This allows us to "build a bridge" from the condensation models to the thermal reduction of the GDN compositions by varying the proportion of dust in the primordial system (*see above*) and searching for optimal condensation conditions for the realization of succeeding chondrule-forming processes. The presence of a reducing agent in this scheme plays no crucial role. The presence of carbon and hydrogen can be reduced to the binding of oxygen produced through the thermal reduction of the system. This is one of the main corollaries of the proposed mechanism of chondrule formation.

The results of our simulations of the thermal reduction for condensates from the gas-dust nebula represent the first attempt in cosmochemistry and meteoritics. The calculations were performed on mineral compositions as the condensation products of the solar nebula at 800–1200 K, that were calculated using the model by Petaev and Wood (2005 – the CWPI code). These model condensates were subjected to "numerical melting" above the olivine liquidus up

to ~1550–2100° C and log $f_{O2} \approx -7$. As a result, we observed a successive release of metal coupled with the formation of a sequence of FeO-depleted and SiO_2-enriched melts demonstrating a monotonous increase in mg#. This is an expected result. The nontrivial corollaries of our calculations concern the model relations between the amount (wt.%) and composition (Ni/(Ni + Fe)) of the metal. They turned out to be identical or close to the observed characteristics of the metal in ordinary LL, L, and H chondrites (Fig. 10). The result obtained is considered as an important argument for the reality of the impulsive heating of protochondritic materials, giving rise to primary metal and complementary silicate spherules of various compositions.

The construction of such polygenetic models opens the possibilities for a systematic study of the effect of the GDN composition and P-T-f_{O2} parameters (including the dust/gas ratios, the degree of fractionation, and the kinetic condensation effects) and the scales of superheating the previously condensed materials on the compositions of the complementary metal and melt ("proto-silicate chondrules"). The results presented can be used to construct more advanced models that allow for the possibility of multiple heating of the initial materials and mixing of the thermal reduction and condensation products. Obviously, the evaporative differentiation processes should also be taken into account here by making allowance for the effects of different evaporation of petrogenic oxides and trace elements during the heating of condensates (*Alexander*, 2004) and the cooling of chondrules. Thus, in prospect, the numerical simulation of a broad spectrum of ordinary and CR chondrites differing in the degree of metal reduction and other petrologic-geochemical characteristics seems to be realistic.

REFERENCES

Alexander, C.M.O'D., Chemical Equilibrium and Kinetic Constraints for Chondrule and CAI Formation Conditions, *Geochim. Cosmochim. Acta*, 2004, vol. 68, pp. 3943–3969.

Anders, E. and Grevesse, N., Abundances of the Elements: Meteoritic and Solar, *Geochim. Cosmochim. Acta*, 1989, vol. 53, pp. 197–214.

Ariskin, A.A. and Barmina, G.S., *Modelirovanie fazovykh ravnovesii pri kristallizatsii bazal'tovykh magm* (Simulation of Phase Equilibria During Crystallization of Basaltic Magmas), Moscow: Nauka, 2000.

Ariskin, A.A., Borisov, A.A., and Barmina, G.S., Simulation of the Equilibrium of Iron-Silicate Melts in Basaltic Systems, *Geokhimiya*, 1992, no. 9, pp. 1231–1240.

Ariskin, A.A., Borisov, A.A., and Petaev, M.I., Calculating Metal-Silicate Equilibria in Meteoritic Igneous Systems, *Abs. LPSC XXVII*, Houston, 1996, pt 1, pp. 37–38.

Ariskin, A.A., Petaev, M I., Borisov, A.A., and Barmina, G.S., METEOMOD: A Numerical Model for the Calculation of Melting-Crystallization Relationships in Meteoritic Igneous Systems, *Meteoritics Planet. Sci.*, 1997, vol. 32, no. 1, pp.. 123–133.

Ariskin, A.A., Yakovlev, O.I., Barmina, G.S., and Bychkov, K.A., Modeling Thermal Reduction of Chondritic Melts Producing Metallic Iron and Residual Silicate Systems, *Abs. 69th Meteoritical Meeting*, Zurich, 2006, #5009.

Ariskin, A.A., Yakovlev, O.I., and Borisov, A.A., On the Possibility of Thermal Metal Reduction when Heating Chondritic Melts, in *Materials of the Seminar on Experimental Mineralogy, Petrology, and Geochemistry*, Moscow: GEOKHI, 1997.

Barmina, G.S., Yaroshevskii, A.A., and Shevaleevskii, I.D., Distribution of Si, Mg, Mn, Ca, and Cr between Olivine Crystal and Peridotite Melts (from Experimental Data). *Geokhimiya*, 1974, no. 5, pp. 773–789.

Berman, R.G., Internally Consistent Thermodynamic Data for Minerals in the System Na_2O-K_2O-CaO-MgO-FeO-Fe_2O_3-Al_2O_3-SiO_2-TiO_2-H_2O-CO_2, *J. Petrol.*, 1988, vol. 29, pp. 445–522.

Bischoff, A., Palme, H., Schultz L., et al., Acfer 182 and Paired Samples, an Iron-Rich Carbonaceous Chondrite: Similarities with ALH85085 and Relationship to CR Chondrites, *Geochim. Cosmochim. Acta*, 1993, vol. 57, pp. 2631–2648.

Borisov, A.A. and Ariskin, A.A., Fe and Ni Solubility in Silicate Melts Equilibrated with Metal, *Abs. LPSC XXVII*, Houston, 1996, pt. 1, pp. 133–134.

Borisov, A.A. and Shapkin, A.I., New Empirical Equation for the Dependence of the Fe^{3+}/Fe^{2+} ratio in Natural Melts on Their Composition, Oxygen Fugacity, and Temperature, *Geokhimiya*, 1989, no. 6, pp. 892–898.

Bouhifd, M.A., Besson, P., Courtial, P., et al., Thermochemistry and Melting Properties of Basalt, *Contrib. Mineral. Petrol.*, 2007, vol. 153, pp. 689–698.

Brett, R. and Sato, M., Intrinsic Oxygen Fugacity Measurements on Seven Chondrites, a Pallasite, and a Tektite and the Redox State of Meteorite Parent Bodies, *Geochim. Cosmochim. Acta*, 1984, vol. 48, pp. 111–120.

Bychkov, K.A., Ariskin, A.A., and Borisov, A.A., Thermodynamic Modeling of Precipitation of Fe-Ni-Metal in Super-Liquidus Chondritic Systems, *Abs. 69th Meteoritical Meeting*, Zurich, 2006, #5010.

Campbell, A.J. and Humayun, M., Formation of Metal in Grosvenor Mountains 95551 and Comparison to Ordinary Chondrites, *Geochim. Cosmochim. Acta*, 2003, vol. 67, pp. 2481–2495.

Campbell, A.J. and Humayun M., Formation of Metal in the CH Chondrites ALH 85085 and PCA 91467, *Geochim. Cosmochim. Acta*, 2004, vol. 68, pp. 3409–3422.

Campbell, A.J., Humayun, M., and Weisberg, M.K., Siderophile Element Constraints on the Formation of Metal in the Metal-Rich Chondrites Bencubbin, Weatherford, and Gujba, *Geochim. Cosmochim. Acta*, 2002, vol. 66, pp. 647–660.

Campbell, I.H., Naldrett, A.J., and Roeder, P L., Nickel Activity in Silicate Liquids: Some Preliminary Results, *Can. Mineral.*, 1979, vol. 17, pp. 495–505.

Campbell, A.J., Zanda, B., Perron, C., et al., Origin and Thermal History of Fe-Ni-Metal in Primitive Chondrites, in *Chondrites and the Protoplanetary Disk*, Krot, A.N., Scott, E.R.D., and Reipurth, B., Eds., ASP Conf. Ser., 2005, vol. 341, pp. 407–431.

Cohen, B.A. and Hewins, R.H., An Experimental Study of the Formation of Metallic Iron in Chondrules, *Geochim. Cosmochim. Acta*, 2004, vol. 68, pp. 1677–1689.

Cohen, B.A., Hewins, R.H., and Alexander, C.M.O'D., The Formation of Chondrules by Open-System Melting of Nebular Condensates, *Geochim. Cosmochim. Acta*, 2004, vol. 68, pp. 1661–1675.

Cohen, B.A., Hewins, R.H., and Yu, Y., Evaporation in the Young Solar Nebula as the Origin of "Just-Right" Melting of Chondrules, *Nature*, 2000, vol. 406, pp. 600–602.

Connoly, H.C.,Jr., Huss, G.R., and Wasserburg, G.J., On the Formation of Fe-Ni-Metal in Renazzo-Like Carbonaceous Chondrites, *Geochim. Cosmochim. Acta*, 2001, vol. 65, pp. 4567–4588.

Dorofeeva, V.A. and Makalkin, A.B., *Evolyutsiya rannei Solnechnoi sistemy. Kosmokhimicheskie i fizicheskie aspekty* (Evolution of the Early Solar System. Cosmochemical and Physical Aspects), Moscow, URSS, 2004.

Doyle, C.D., Prediction of the Activity of FeO in Multicomponent Magma from Known Values in [SiO_2-$KAlO_2$-$CaAl_2Si_2O_8$]-FeO Liquids, *Geochim. Cosmochim. Acta*, 1988, vol. 52, pp. 1827–1834.

Doyle, C.D. and Naldrett, A.J., Ideal Mixing of Divalent Cations in Mafic Magma and Its Effect on the Solution of Ferrous Oxide, *Geochim. Cosmochim. Acta*, 1986, vol. 50, pp. 435–443.

Ebel, D.S., Model Evaporation of FeO-Bearing Liquids: Application to Chondrules, *Geochim. Cosmochim. Acta*, 2005, vol. 69, pp. 3183–3193.

Ebel, D.S. and Grossman, L., Condensation in Dust-Enriched Systems, *Geochim. Cosmochim. Acta*, 2000, vol. 64, pp. 339–366.

Frenkel, M.Ya., Yaroshevskii, A.A., Ariskin, A.A., et al., *Dinamika vnutrikamernoi differentsiatsii bazitovykh magm* (Dynamics of Intrachamber Differentiation of Basite Magmas), Moscow: Nauka, 1988.

Ghiorso, M.S., Hirschmann, M.M., Reiners, P.W., and Kress, V.C., III, The pMELTS: A Revision of MELTS for Improved Calculation of Phase Relations and Major Element Partitioning Related to Partial Melting of the Mantle to 3 GPa, *Geochem. Geophys. Geosyst.*, 2002, vol. 3 (5), doi: 10.1029/2001GC000217.

Ghiorso, M.S. and Sack, R.O., Chemical Mass Transfer in Magmatic Processes IV. A Revised and Internally Consistent Thermodynamic Model for the Interpolation and Extrapolation of Liquid–Solid Equilibria in Magmatic Systems at Elevated Temperatures and Pressures, *Contrib. Mineral. Petrol.*, 1995, vol. 119, pp. 197–212.

Grossman, L. and Olsen, E., Origin of the High-Temperature Fraction of C2 Chondrites, *Geochim. Cosmochim. Acta*, 1974, vol. 38, pp. 173–187.

Grossman, J.N. and Wasson, J.T., The Origin and History of the Metal and Sulfide Components of Chondrules, *Geochim. Cosmochim. Acta*, 1985, vol. 49, pp. 925–939.

Hanon, P., Robert, F., and Chaussdion, M., High Carbon Concentrations in Meteoritic Chondrules, *Geochim. Cosmochim. Acta*, 1998, vol. 62, pp. 903–913.

Holzheid, A., Borisov, A., and Palme, H., The Effect of Oxygen Fugacity and Temperature on Solubilities of Nickel, Cobalt, and Molybdenum in Silicate Melts, *Geochim. Cosmochim. Acta*, 1994, vol. 58, pp. 1975–1981.

Jones, R.H., Petrology of FeO-Poor, Porphyritic Pyroxene Chondrules in the Semarkona Chondrite, *Geochim. Cosmochim. Acta*, 1994, vol. 58, pp. 5325–5340.

Jones, R.H. and Palme, H., Geochemical Constraints on the Origin of the Earth and Moon, in *Origin of the Earth and Moon*, Eds. Canup, R.M. and Righter, K., Eds., Tuscon: University of Arizona Press, 2000, pp. 197–216.

Jurewicz, A.J.G., Mittlefehldt, D.W., and Jones, J.H., Experimental Partial Melting of the St. Severin (LL) and Lost City (H) Chondrites, *Geochim. Cosmochim. Acta*, 1995, vol. 59, pp. 391–408.

Kallemeyn, G.W., Rubin, A.E., and Wasson, J.T., Compositional Studies of Bencubbin Dark Silicate Host and an OC Clast: Relationships to Other Meteorites and Implications for Their Origin, *Lunar Planet. Sci.*, 2001, vol. 32, #2070.

King, E.A., Refractory Residues, Condensates and Chondrules from Solar Furnace Experiments, *J. Geophys. Res.*, 1982, vol. 87, pp. A429–434.

King, E.A., Reduction, Partial evaporation, and Spattering: Possible Chemical and Physical Processes in Fluid Drop Chondrules Formation, in *Chondrules and Their Origin*, 1984, pp. 180–187.

Kong, P. and Ebihara, M., The Origin and Nebular History of the Metallic Phase of Ordinary Chondrites, *Geochim. Cosmochim. Acta*, 1997, vol. 61, pp. 2317–2329.

Krot, A.N., Keil, K., Goodrich, C.A., et al., Classification of Meteorites, in *Meteorites, Comets, and Planets* (Treatise on Geochemistry), Oxford: Elsevier-Pergamon, 2003, vol. 1, pp. 83–128.

Kong, P. and Palme, H., Compositional and Genetic Relationship between Chondrules, Chondrule rims, Metal, and Matrix in the Renazzo Chondrite, *Geochim. Cosmochim. Acta*, 1999, vol. 63, pp. 3673–3682.

Lee, M.S., Rubin, A.E., and Wasson, J.T., Origin of Metallic Fe-Ni in Renazzo and Related Chondrites, *Geochim. Cosmochim. Acta*, 1992, vol. 56, pp. 2521–2533.

Libourel, G., Krot, A.N., and Tissandier, L., Role of Gas-Melt Interaction during Chondrule Formation, *Earth Planet. Sci. Lett.*, 2006, vol. 251, pp. 232–240.

Lodders, K., Solar System Abundances and Condensation Temperatures of the Elements, *Astrophys. J.*, 2003, vol. 591, pp. 1220–1247.

McSween, H.Y., Jr. and Labotka, T.C., Oxidation during Metamorphism of the Ordinary Chondrites, *Geochim. Cosmochim. Acta*, 1993, vol. 57, pp. 1105–1114.

Myers, J. and Eugster, H.P., The System Fe-Si-O: Oxygen Buffer Calibrations to 1.500 K, *Contrib. Mineral. Petrol.*, 1983, vol. 82, pp. 75–90.

Nagahara, H., Reduction Kinetics of Olivine and Oxygen Fugacity Environment during Chondrule Formation, Abs. *17th Lunar Planet. Sci. Conf.*, 1986, pp. 595–596.

Petaev, M.I. and Wood, J.A., Meteoritic Constraints on Temperatures, Pressures, Cooling Rates, Chemical Compositions, and Modes of Condensation in the Solar Nebula, in *Chondrites and the Protoplanetary Disk*, Krot, A.N., Scott, E.R.D, and Reipurth, B., Eds., ASP Conf. Ser., 2005, vol. 341, pp. 373–406.

Petaev, M.I., Wood, J.A., Meibom, A., et al., The ZONMET Thermodynamic and Kinetic Model of Metal Condensation, *Geochim. Cosmochim. Acta*, 2003, vol. 67, pp. 1737–1751.

Prior, G.T., On the Genetic Relationship and Classification of Meteorites, *Miner. Magazine*, 1916, vol. 18, pp. 26–43.

Righter, K., Metal–Silicate Partitioning of Siderophile Elements and Core Formation in the Early Earth, *Ann. Rev. Earth Planet. Sci.*, 2003, vol. 31, pp. 135–174.

Roeder, P.L., Activity of Iron and Olivine Solubility in Basaltic Liquids, *Earth Planet. Sci. Lett.*, 1974, vol. 23, pp. 397–410.

Rubin, A.E., Petrologic, Geochemical and Experimental Constraints on Models of Chondrule Formation, *Earth Sci. Rev.*, 2000, vol. 50, pp. 3–27.

Rubin, A.E., Fegley, B., and Brett, R., Oxidation State of Chondrites, in *Meteorites and the Early Solar System*, Kerridge, J.F. and Matthews, M.S., Eds., Arizona: University of Arizona, 1988, pp. 488–511.

Schaefer, L. and Fegley, B., Jr., Outgassing of Ordinary Chondritic Material and Some of Its Implications for the Chemistry of Asteroids, Planets, and Satellites, *Icarus*, 2007, vol. 186, pp. 462–483.

Schmitt, W., Palme, H., and Wanke, H., Experimental Determination of Metal/Silicate Partition Coefficients for P, Co, Ni, Cu, Ga, Ge, MO, and W and Some Implications for the Early Evolution of the Earth, *Geochim. Cosmochim. Acta*, 1989, vol. 53, pp. 173–185.

Sears, D.W.G., Huang, S., and Benoit, P.H., Open-System Behavior during Chondrule Formation, in *Chondrules and the Protoplanetary Disk*, Hewins, R.H., Jones, R.H., and Scott, E.R.D., Eds, Cambridge: Cambridge Univ. Press, 1996, pp. 221–231.

Shapkin, A.I. and Sidorov, Yu.I., *Termodinamicheskie modeli v kosmokhimii i planetologii* (Thermodynamic Models in Cosmochemistry and Planetology), Moscow: URSS, 2004.

Simonenko, A.M., *Asteroidy* (Asteroids), Moscow: Nauka, 1985.

Snyder, D.A. and Carmichael, I.S.E., Olivine-Liquid Equilibria and the Chemical Activities of FeO, NiO, Fe_2O_3, and MgO in Natural Basic Melts, *Geochim. Cosmochim. Acta*, 1992, vol. 56, pp. 303–318.

Swartzendruber, L.J., Itkin, V.P., and Alcock, C.B., The Fe-Ni (Iron-Nickel) System, *J. Phase Equilibria*, 1991, vol. 12, pp. 288–312.

Tomiska, J. and Neckel, A., Thermodynamics of Solid Fe-Ni Alloys – Mass-Spectrometric Determination of Thermodynamic Mixing Effects and Calculation of the Phase Diagram Ber. Bunsenges, *Phys. Chem.*, 1985, vol. 89, pp. 1104–1109.

Trieloff, M. and Palme, H., Early Solar System Chronology in Astrophysical Context, *Abs. 69th Meteoritical Meeting*, Zurich, 2006, #5084.

Varela, M.E., Kurat, G., and Zinner, E., The Primary Liquid Condensation Model and the Origin of Barred Olivine Chondrules, *Icarus*, 2006, vol. 184, pp. 344–364.

Walte, M.J., Newsom, H.E., Ertel, W., and Holzheid, A., Siderophile Elements in the Earth and Moon: Metal-Silicate Partitioning and Implications for Core Formation, in *Origin of the Earth and Moon*, Canup, R.M and Righter, K., Eds., Tuscon: University of Arizona Press, 2000, pp. 265–289.

Weisberg, M.K., Prinz, M., Clayton, R.N., and Mayeda, T.K., The CR (Renazzo-Type) Carbonaceous Chondrite Group and Its Implications, *Geochim. Cosmochim. Acta*, 1993, vol. 57, pp. 1567–1586.

Weisberg, M.K., Prinz, M., Clayton, R.N., et al., A New Metal-Rich Chondrite Group-Let, *Meteorit. Planet. Sci.*, 2001, vol. 36, pp. 401–418.

Wood, J.A. and Hashimoto, A., Mineral Equilibrium in Fractionated Nebular Systems, *Geochim. Cosmochim. Acta*, 1993, vol. 57, pp. 2377–2388.

Yakovlev, O.I., Ariskin, A.A., Barmina, G.S., and Bychkov, K A., Modeling Fe-Ni-Metal and Silicate Melt Compositions Produced by Thermal Reduction of Nebular Condensates above the Liquidus, *Abs. Annual Goldschmidt Conf.*, Vancuver, Canada, 2008.

Yakovlev, O.I., Dikov, Yu.P., Gerasimov, M.V., et al., Experimental Study of Factors Determining the Composition of Lunar Regolith Glasses, *Geokhimiya*, 2003, no. 5, pp. 467–481.

Yakovlev, O.I., Markova, O.M., Belov, A.N., and Semenov, G.A., On the Formation of Metallic Iron when Heating Chondrites, *Meteoritika*, 1987, no. 46, pp. 104–118.

Yakovlev, O.I., Markova, O.M., Belov, A.N., and Semenov, G.A., The Compositional Evolution of Meteorites Produced by the Vaporization of Iron, *Abs. 16th Lunar Planet. Sci. Conf.*, 1985, pp. 928–929.

Zanda, B., Hewins, R.H., Bourot-Denise, M., et al., Formation of Solar Nebula Reservoirs by Mixing Chondritic Components, *Earth Planet. Sci. Lett.*, 2006, vol. 248, pp. 650–660.